

Reduced adenosine-to-inosine miR-455-5p editing promotes melanoma growth and metastasis

Einav Shoshan^{1,11}, Aaron K. Mobley^{1,11}, Russell R. Braeuer¹, Takafumi Kamiya¹, Li Huang¹, Mayra E. Vasquez¹, Ahmad Salameh², Ho Jeong Lee¹, Sun Jin Kim¹, Cristina Ivan³, Guermarie Velazquez-Torres¹, Ka Ming Nip⁴, Kelsey Zhu⁴, Denise Brooks⁴, Steven J. M. Jones⁴, Inanc Birol⁴, Maribel Mosqueda⁵, Yu-ye Wen⁵, Agda Karina Eterovic⁵, Anil K. Sood^{1,3}, Patrick Hwu⁶, Jeffrey E. Gershenwald⁷, A. Gordon Robertson⁴, George A. Calin⁸, Gal Markel^{9,10}, Isaiah J. Fidler¹ and Menashe Bar-Eli^{1,12}

Although recent studies have shown that adenosine-to-inosine (A-to-I) RNA editing occurs in microRNAs (miRNAs), its effects on tumour growth and metastasis are not well understood. We present evidence of CREB-mediated low expression of ADAR1 in metastatic melanoma cell lines and tumour specimens. Re-expression of ADAR1 resulted in the suppression of melanoma growth and metastasis *in vivo*. Consequently, we identified three miRNAs undergoing A-to-I editing in the weakly metastatic melanoma but not in strongly metastatic cell lines. One of these miRNAs, miR-455-5p, has two A-to-I RNA-editing sites. The biological function of edited miR-455-5p is different from that of the unedited form, as it recognizes a different set of genes. Indeed, wild-type miR-455-5p promotes melanoma metastasis through inhibition of the tumour suppressor gene *CPEB1*. Moreover, wild-type miR-455 enhances melanoma growth and metastasis *in vivo*, whereas the edited form inhibits these features. These results demonstrate a previously unrecognized role for RNA editing in melanoma progression.

Melanoma is the most aggressive type of skin cancer. In 2014, an estimated 76,100 new cases of melanoma were diagnosed in the United States, and 9,710 will result in death¹. One important step for progression to metastatic disease is the transition from the radial growth phase to the vertical growth phase². Previous reports from our laboratory have shown that cyclic AMP-responsive element (CRE) binding protein (CREB) regulates many important functions during this transition^{3,4}, including acting as a survival factor and increasing cell invasion by regulating MMP2, IL8, BCL2, MCAM (also known as MUC18) and the tumour suppressor CYR61 (refs 5–8). Furthermore, CREB regulates other important transcription factors involved in melanoma progression, such as MITF and AP2 α (refs 9,10). Herein, we identified an important and previously unknown target for CREB, the RNA-editing enzyme adenosine deaminase acting on RNA 1 (ADAR1, also known as ADAR).

RNA editing, as well as other post-transcriptional modifications, increases protein diversity from a limited set of genes and can create proteins with several different functions from the same pre-messenger RNA. In cancer cells, this process can promote tumour growth and progression^{11,12}. During RNA editing, a site-specific alteration in the RNA sequence occurs and is then copied to the DNA sequence, excluding capping, polyadenylation or splicing¹³. The most common form of RNA editing is adenosine-to-inosine (A-to-I) editing, which is mediated by the action of ADAR enzymes^{14–16}. The translational machinery then reads the inosine as guanosine, leading to altered amino-acid sequences, a shift in the codon reading frame or, if the editing occurs in a non-coding region, a disruption in the stability of the RNA transcript^{17–20}. More recently, ADAR-mediated RNA editing has been shown to occur in regulatory RNAs such as microRNAs (miRNAs), and can interfere

¹Department of Cancer Biology, Unit 0173, The University of Texas MD Anderson Cancer Center, 1515 Holcombe Blvd., Houston, Texas 77030, USA. ²The University of Texas Health Science Center at Houston, 1825 Pressler Street, Houston, Texas 77030, USA. ³Department of Gynecologic Oncology, Unit 1362, The University of Texas MD Anderson Cancer Center, 1515 Holcombe Blvd., Houston, Texas 77030, USA. ⁴Canada's Michael Smith Cancer Agency, Vancouver, British Columbia V5Z 4S6, Canada. ⁵Institute of Personalized Cancer Therapy, The University of Texas MD Anderson Cancer Center, 1515 Holcombe Blvd., Houston, Texas 77030, USA. ⁶Department of Melanoma Medical Oncology, Unit 0430, The University of Texas MD Anderson Cancer Center, 1515 Holcombe Blvd., Houston, Texas 77030, USA. ⁷Department of Surgical Oncology, Unit 1484, The University of Texas MD Anderson Cancer Center, 1515 Holcombe Blvd., Houston, Texas 77030, USA. ⁸Department of Experimental Therapeutics, Unit 1950, The University of Texas MD Anderson Cancer Center, 1515 Holcombe Blvd., Houston, Texas 77030, USA. ⁹Ella Institute of Melanoma, Sheba Medical Center, Ramat-Gan 52621, Israel. ¹⁰Clinical Microbiology and Immunology, Sackler Faculty of Medicine, Tel Aviv University, Ramat Aviv 69978, Israel. ¹¹These authors contributed equally to this work.

¹²Correspondence should be addressed to M.B.-E. (e-mail: mbareli@mdanderson.org)

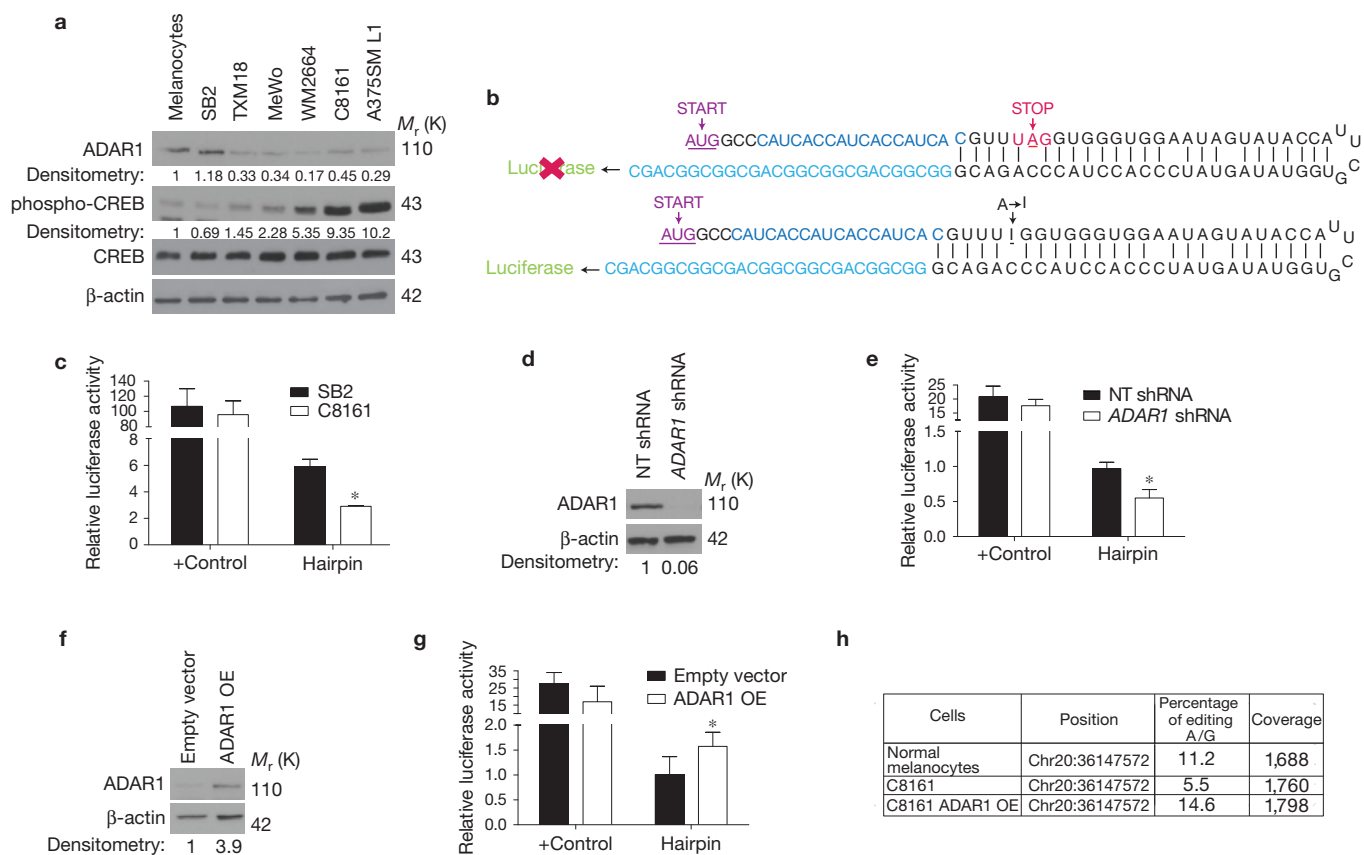


Figure 1 ADAR1 expression and function is lost in metastatic melanoma. **(a)** Western blot analysis of a panel of melanoma cell lines shows decreased ADAR1 expression in highly metastatic cell lines. An inverse correlation is observed between ADAR1 expression and phospho-CREB expression, whereas total CREB expression is similar in all cell lines (data are representative of three biologically independent experiments). **(b)** Schematic representation of ADAR1 A-to-I RNA-editing hairpin loop luciferase reporter. The stop codon leads to no luciferase expression (top panel), whereas A-to-I editing within the stop codon leads to increased expression (bottom panel). **(c)** Luciferase activity from the hairpin luciferase construct decreases more than twofold in C8161 cells when compared with SB2 cells (right side of figure), $*P < 0.05$. The positive control shows similar levels between the two cell lines (left side of figure). Positive controls represent the constantly active form of the hairpin in which the stop codon was mutated to the edited form. **(d)** ADAR1 shRNA transduction leads to ~95% reduction in ADAR1 expression in SB2

cells, as shown by western blot analysis (data are representative of three biologically independent experiments). **(e)** Hairpin luciferase activity is decreased on silencing of ADAR1 in SB2 cells, $*P < 0.05$. **(f)** Western blot analysis of overexpression of ADAR1 in C8161 cells indicates a fourfold increase in ADAR1 expression when compared with empty vector control (data are representative of three biologically independent experiments). **(g)** Hairpin luciferase activity is increased after overexpression of ADAR1 in C8161 cells, $*P < 0.05$. **(h)** Results of *BLCAP* editing by ADAR1. *BLCAP* is a known substrate for ADAR1 editing activity^{24,33,34}. Metastatic melanoma C8161 cells have significantly lower editing rate (percentage) when compared with normal melanocytes. Overexpressing ADAR1 in C8161 rescued the editing percentage about threefold. Each experiment in **c**, **e** and **g** is the result of $n = 3$ biologically independent samples per group; error bars represent s.d. Statistical significance was determined by a two-tailed Student *t*-test. Uncropped images of the blots are shown in Supplementary Fig. 8.

with miRNA biogenesis, alter their stability within the cell or alter their target binding^{21–23}.

Here, we found that CREB negatively regulates ADAR1 and that ADAR1 inhibits melanoma tumour growth and metastasis. Moreover, we identified two ADAR1-mediated A-to-I RNA-editing sites in miR-455-5p as well as binding targets for the wild-type (WT) and the A-to-I edited version of miR-455-5p. Indeed, the WT but not the edited form specifically targets the tumour suppressor gene *CPEB1*. Furthermore, WT miR-455-5p enhances melanoma growth and metastasis *in vivo*, whereas the edited form inhibits these features. These results provide a key missing link in the mechanistic understanding of the role of RNA editing in the acquisition of the melanoma metastatic phenotype.

RESULTS

ADAR1 expression decreases with melanoma progression

To further evaluate the role of ADAR1 in melanoma progression, we determined the ADAR1 protein expression levels in established highly metastatic human melanoma cell lines (TXM18, MeWo, WM2664, C8161 and A375SML1), a melanoma cell line with low metastatic potential (SB2) and normal melanocytes through western blot analysis. ADAR1 expression was significantly lower in all the highly metastatic melanoma cell lines than in the SB2 cells and normal melanocytes (Fig. 1a, top panel). Collectively, these data demonstrate that ADAR1 expression is reduced in metastatic melanoma cell lines and in clinical metastatic melanoma specimens²⁴ during melanoma progression.

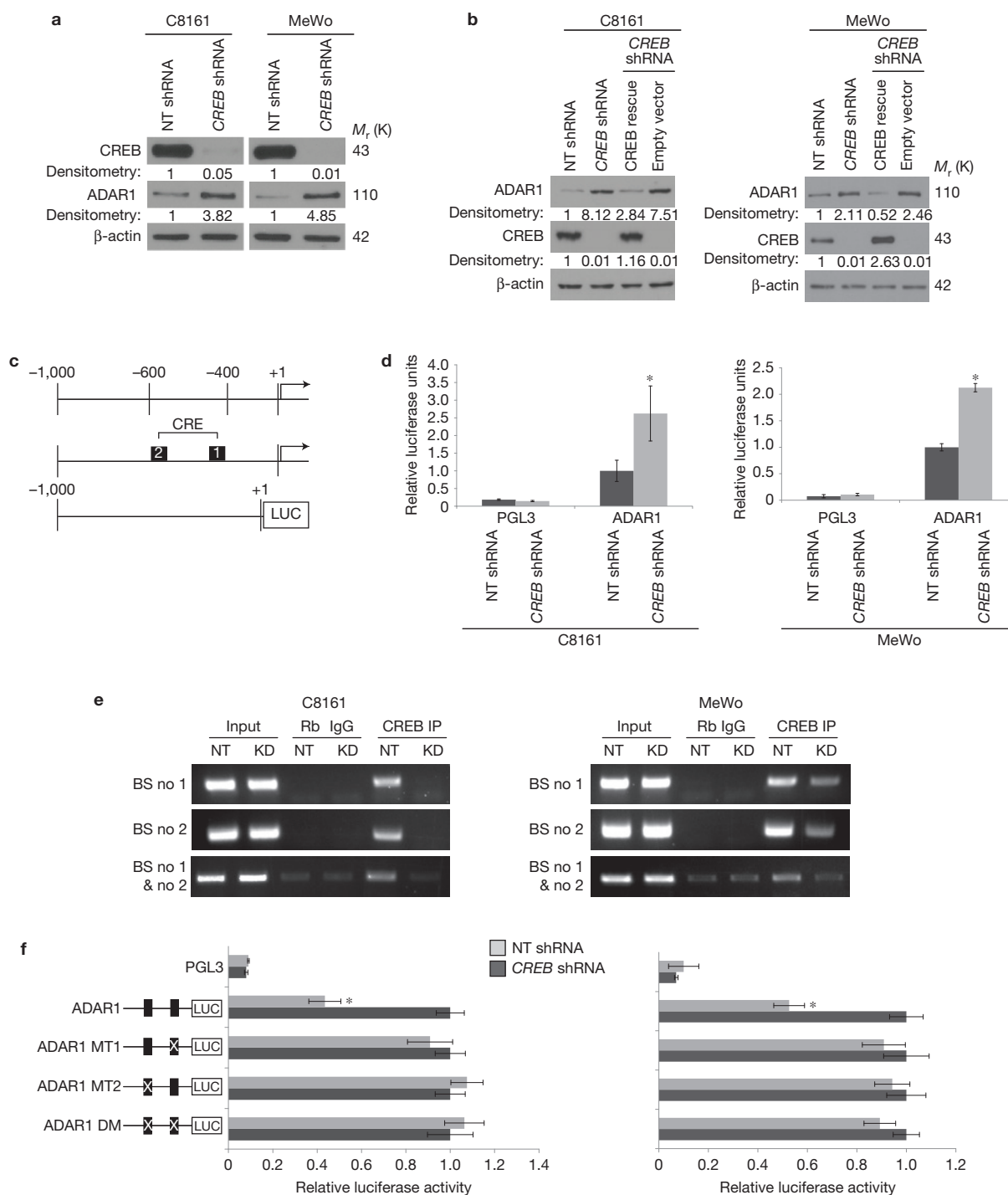


Figure 2 CREB negatively regulates ADAR1 expression. **(a)** Western blot analysis of CREB shRNA transduced C8161 and MeWo cells shows a three- to fivefold increase in ADAR1 expression as compared with NT shRNA controls (data are representative of three biologically independent experiments). **(b)** Rescue of CREB expression in the CREB-silenced cells results in downregulation of ADAR1 expression in both C8161 and MeWo cells (data are representative of three biologically independent experiments). **(c)** Schematic representation of the ADAR1 promoter region fused to the luciferase reporter gene and its predicted CRE binding sites. **(d)** ADAR1 promoter driven luciferase expression increased twofold after CREB silencing as compared with the NT control, $*P < 0.01$ ($n = 3$ biologically independent samples per group, statistical significance was determined by two-tailed Student *t*-test; error bars represent s.d.). **(e)** ChIP analyses showed no

binding of CREB to the ADAR1 promoter at either CRE binding site (BS) after CREB silencing in either C8161 or MeWo cell lines. IgG antibodies were used as negative controls. Input DNA was used as a loading control (data are representative of three biologically independent experiments). Statistical significance was determined by a two-tailed Student *t*-test. **(f)** Schematic representation of the ADAR1 promoter point mutations (left of the panel). Luciferase activity driven by the ADAR1 promoter increased in the NT shRNA group when mutations were made at either or both of the CRE binding sites for both C8161 (left) and MeWo (right), $*P < 0.01$ ($n = 3$ biologically independent samples per group, statistical significance was determined by a two-tailed Student *t*-test; error bars represent s.d.). Uncropped images of blots and gels are shown in Supplementary Fig. 8.

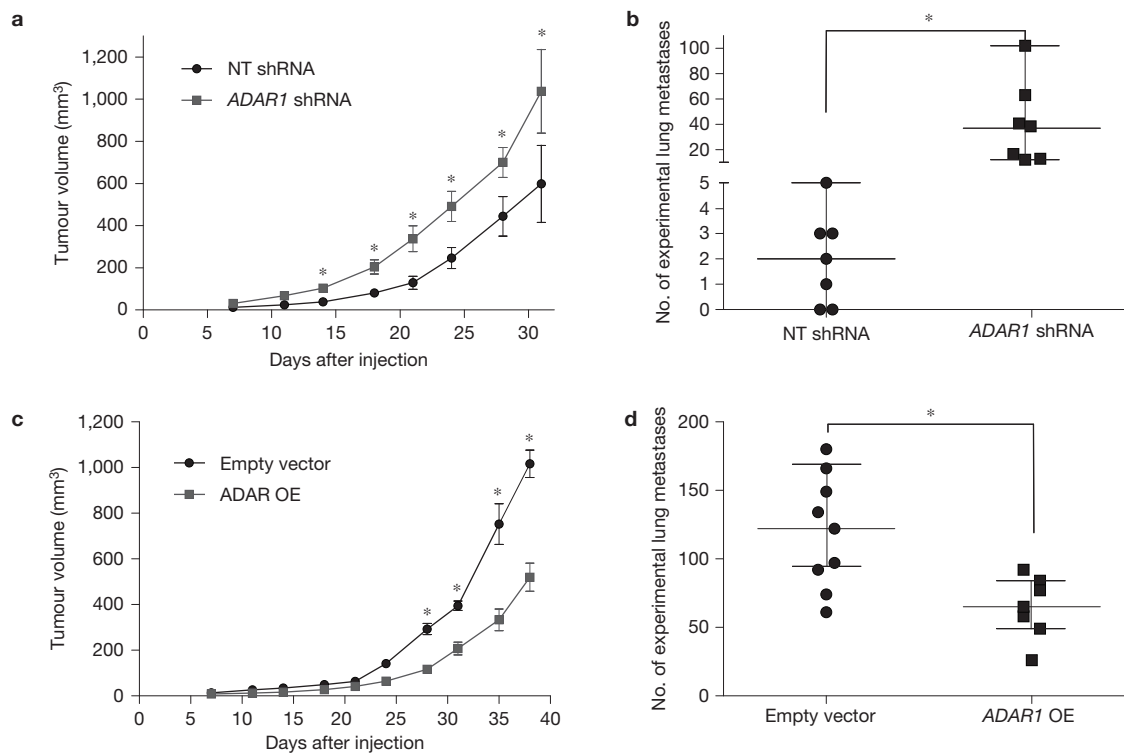


Figure 3 ADAR1 expression leads to decreased melanoma tumour growth and metastasis. (a) Effect of *ADAR1* silencing in SB2 cells on subcutaneous tumour growth. *ADAR1* silencing led to a significant increase in tumour growth, $*P < 0.05$ ($n = 10$ mice in each group; two-tailed Student *t*-test; error bars represent s.d.). (b) Effect of *ADAR1* silencing on metastatic potential of melanoma cells. An increase in the number of experimental lung metastases was observed in mice injected with *ADAR1*-silenced SB2 cells as compared with NT shRNA injected control mice, $*P < 0.01$ ($n = 7$ mice in each group; statistical significance was determined by a two-tailed Student *t*-test; error

bars represent s.d.). (c) Effect of *ADAR1* OE in C8161 cells on subcutaneous tumour growth. *ADAR1* OE led to a significant decrease in tumour growth, $*P < 0.05$ ($n = 10$ mice in each group; two-tailed Student *t*-test; error bars represent s.d.). (d) Effect of *ADAR1* OE on metastatic potential of melanoma cells. A significant decrease in the number of experimental lung metastases was observed in mice injected with *ADAR1* overexpressing C8161 cells as compared with empty vector injected control mice, $*P < 0.01$ (empty vector, $n = 9$ mice; *ADAR1* OE, $n = 7$ mice). Statistical significance by two-tailed Student *t*-test; error bars represent s.d.

RNA-editing activity of ADAR decreases with melanoma progression

We next sought to determine whether the RNA-editing activity of ADAR1 was affected. In this construct, the stop codon (UAG) prevents luciferase expression, whereas an A-to-I editing event within the stop codon leads to luciferase expression (Fig. 1b). Using these luciferase constructs, we found that the ability of highly metastatic C8161 cells to carry out A-to-I editing was lower (by 50%) than that of low metastatic potential SB2 cells (Fig. 1c).

Next, *ADAR1* was stably silenced in the low metastatic potential SB2 cells using a lentiviral *ADAR1*-targeted short hairpin RNA (shRNA) construct. Western blot analysis revealed that ADAR1 protein expression was knocked down by more than 95% when compared with the non-targeting (NT) shRNA (Fig. 1d). Furthermore, *ADAR1* was overexpressed (*ADAR1* OE) in highly metastatic C8161 cells (which express low levels of ADAR1). *ADAR1* expression was nearly four times higher in the *ADAR1* OE cells than in the empty vector control (Fig. 1f). Using the hairpin luciferase construct to assess the RNA-editing ability of these cells, we confirmed that silencing of *ADAR1* in SB2 cells or overexpression of *ADAR1* in C8161 cells decreased or increased the A-to-I RNA-editing activity, respectively (Fig. 1e,g). We also analysed the editing rate of *BLCAP* mRNA (a

known substrate for ADAR1 editing²⁵) and confirmed that the C8161 cells had less than 50% ability to carry out A-to-I editing when compared with normal melanocytes. Re-expression of ADAR1 in C8161 cells (*ADAR1* OE) rescued their ability to carry out A-to-I editing (Fig. 1h). These results confirmed that the RNA-editing activity of ADAR1 is functional in melanoma cells and that the loss of ADAR1 in metastatic melanoma leads to a decrease in A-to-I RNA editing.

CREB acts as a negative regulator of ADAR1 expression in melanoma

Next, we sought to identify the mechanism(s) by which ADAR1 expression is regulated in melanoma. Gene expression profiling data indicated a two- to threefold increase in ADAR1 expression after *CREB* silencing in metastatic melanoma cells. To validate these findings, a panel of melanoma cell lines was analysed through Western blotting for both ADAR1 and phosphorylated CREB expression. The data revealed an inverse correlation between activated CREB and ADAR1 expression. In the normal melanocytes and low metastatic potential SB2 cells ADAR1 expression was high but phospho-CREB was low, whereas in the highly metastatic cell lines phospho-CREB was high and ADAR1 expression was low (Fig. 1a). Next, we stably silenced *CREB* using shRNA in the highly metastatic C8161 and

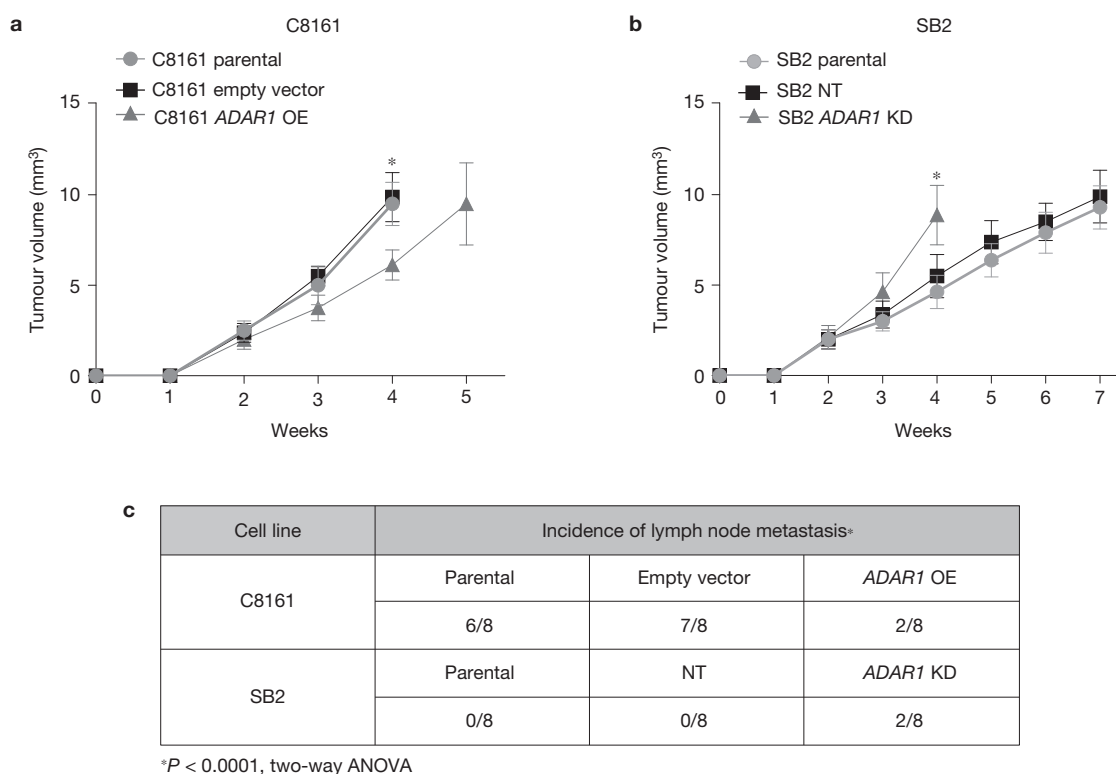


Figure 4 Spontaneous metastasis of SB2 and C8161 melanoma cells. (a) Tumour growth in the skin ridge of the external ear is reduced after overexpression of *ADAR1* in C8161 melanoma cells when compared with the empty vector control ($n=8$ mice in each group; statistical significance was determined by two-way analysis of variance (ANOVA) test, $*P < 0.0001$; error bars represent s.d.). (b) SB2 cells grow at a faster rate in the skin ridge of the external ear when *ADAR1* is silenced. Measurements of tumour growth

from groups C8161 empty vector and SB2 *ADAR1* KD were stopped in week 4 owing to tumour size ($n=8$ mice in each group; statistical significance was determined by two-way ANOVA test, $*P < 0.0001$; error bars represent s.d.). (c) Overexpression of *ADAR1* in C8161 melanoma cells reduced the number of lymph node metastases, whereas silencing *ADAR1* enabled two SB2 tumours to locally metastasize to regional lymph nodes ($n=8$ mice in each group; two-way ANOVA test; $*P < 0.0001$; error bars represent s.d.).

MeWo melanoma cell lines. *CREB* was knocked down by more than 95% in both cell lines when compared with the NT control (Fig. 2a). Silencing of *CREB* in these cells resulted in a three- to fivefold upregulation of *ADAR1*, thus corroborating the complementary DNA expression data (Fig. 2a). To confirm that these findings were specific to *CREB* and not an off-target effect of the shRNA, *CREB* expression was rescued in both silenced cell lines. Rescue of *CREB* indeed restored *CREB* expression and resulted in decreased *ADAR1* expression in both cell lines (Fig. 2b). Silencing of *CREB* in C8161 or overexpressing *CREB* in SB2 cells did not affect the expression of *ADAR2* in these cells (Supplementary Fig. 1).

The promoter region of *ADAR1* contains two *CREB* binding sites within 600 base pairs (bp; -403 and -549) from the translation initiation site A (Fig. 2c). *CREB* silencing increased *ADAR1* luciferase promoter activity two- to threefold in both cell lines, indicating regulation at the transcriptional level (Fig. 2d). Binding of *CREB* at positions -403 and -549 was analysed by chromatin immunoprecipitation (ChIP). Decreased binding of *CREB* was detected at both binding sites following *CREB* silencing in both cell lines (Fig. 2e). Single-point mutations were made at the two *CREB* binding sites individually or in combination in the *ADAR1* promoter luciferase construct. Mutations in the *CREB* binding sites individually or together led to an increase in luciferase expression in the NT shRNA

group to levels similar to those in the *CREB* shRNA in both cell lines (Fig. 2f). Taken together, these data reveal a new role for *CREB*: negative regulation of *ADAR1* and RNA editing.

Suppression of *ADAR1* contributes to tumorigenicity and metastatic potential of melanoma

To elucidate the role of *ADAR1* in melanoma tumorigenicity, we used the *ADAR1*-silenced SB2 cells and the *ADAR1* OE C8161 cells (Fig. 1d,f) and analysed their abilities to produce subcutaneous tumours and experimental lung metastasis *in vivo*. When *ADAR1*-silenced SB2 cells were injected subcutaneously into nude mice, a significant increase in tumour growth was observed when compared with NT shRNA SB2 cells (Fig. 3a). Also, when *ADAR1* OE C8161 cells were injected subcutaneously into nude mice, tumour growth was significantly inhibited when compared with control mice (Fig. 3c). Furthermore, when *ADAR1* knockdown (KD) SB2 cells were injected intravenously, an increase in the median number of experimental lung metastases was observed when compared with the NT shRNA control (*ADAR* KD 37, NT shRNA 2; $P < 0.01$; Fig. 3b). Overexpression of *ADAR1* in C8161 cells injected intravenously led to a significant decrease in the median number of lung metastases when compared with the control mice that received the empty vector $P < 0.01$ (Fig. 3d).

ADAR1 expression inhibits spontaneous metastasis

We next determined the role of ADAR1 in spontaneous melanoma metastasis. To this end, another murine model was used, whereby melanoma cells were injected into the skin ridge of the external ear, and then local lymph node metastasis were monitored. SB2 and C8161 melanoma cells were first transduced with the luciferase gene, and then *ADAR1* was silenced or overexpressed. C8161 Luc/empty vector or Luc/*ADAR1* OE and SB2 Luc/NT shRNA or Luc/*ADAR1* shRNA transduced melanoma cells were injected into the skin ridge of the external ear. Overexpression of *ADAR1* in C8161 melanoma cells significantly decreased tumour growth (Fig. 4a). Silencing *ADAR1* in SB2 cells resulted in increased tumour growth (Fig. 4b). The tumours were then completely resected along with the ear, and metastases to the regional lymph nodes were monitored. In C8161 melanoma cells, six of eight parental and seven of eight Luc/empty vector tumours generated regional lymph node metastasis. *ADAR1* OE in C8161 melanoma cells decreased the incidence of lymph node metastasis (2/8 mice; Fig. 4c and Supplementary Fig. 2). Of the mice injected with low metastatic potential SB2 cells (both the SB2 parental and Luc/NT shRNA transduced groups), none (0/8) developed lymph node metastasis. However, in the Luc/*ADAR1*-silenced group, two of eight mice developed lymph node metastasis (Fig. 4c and Supplementary Fig. 2). Collectively, these results demonstrated that loss of ADAR1 directly contributed to an increase in melanoma growth and metastasis.

miRNA-455-5p is edited by ADAR1

We next sought to determine how loss of ADAR1 from metastatic melanoma affects A-to-I RNA editing in miRNAs and whether the altered editing affects their function and contributes to melanoma metastasis. First, to identify potentially edited miRNAs, two separate miRNA expression arrays were analysed: data from the array of SB2 cells after *ADAR1* silencing and from C8161 cells after *CREB* silencing (Fig. 2a). We identified changes in the expression of 131 miRNAs following *ADAR1* silencing (Supplementary Table 3 of ref. 24) and changes in 239 miRNAs after *CREB* silencing (Supplementary Fig. 3A). Only 12 were common in both arrays (Supplementary Table 1 marked in yellow, Supplementary Fig. 3A). Next, we sequenced the pri-miRNA (the miRNA stem-loop in the context of the primary RNA) of these 12 identified miRNAs using high-throughput sequencing. Among these 12 miRNAs, A-to-I RNA editing was identified in miR-378-3p, miR-324-5p and miR-455-5p (Supplementary Fig. 3B highlighted in yellow). We will concentrate on miR-455-5p, as two ADAR1-mediated A-to-I RNA editing sites were identified (Fig. 5a). The A-to-I RNA-editing sites in miR-378-3p and miR-324-5p are shown in Supplementary Fig. 4. SB2 cells transduced with *ADAR1* shRNA had a decrease in the guanine peak at both sites when compared with the NT shRNA control, indicating a decrease in A-to-I editing (Fig. 5b, black peak under arrows). *ADAR1* OE C8161 cells showed an increase in the guanine peak at both sites when compared with the empty vector control, indicating an increase in A-to-I editing (Fig. 5c). After confirming that the changes in RNA editing were ADAR1 dependent, we determined whether the changes in RNA editing were also CREB dependent. To this end, *CREB*-silenced C8161 and *CREB*-silenced cells transduced with a CREB rescue vector were sequenced. Indeed, on silencing of *CREB* we

observed an increase in A-to-I RNA editing at both sites, and on rescue of CREB expression a decrease in editing was found at these sites, back to levels similar to those in the NT shRNA control (Fig. 5d). Taken together, A-to-I RNA editing occurs in the non-metastatic SB2 cells but not in the C8161 metastatic cells. No editing was found at the DNA level.

To determine whether RNA editing in miR-455-5p affects the miRNA biogenesis, pri-miRNA and mature levels were measured in SB2 *ADAR1* KD and C8161 *CREB* KD cells using real-time PCR (rtPCR). When pri-miRNA-455 levels were analysed, no significant differences were observed in either SB2 or C8161 cells after *ADAR1* KD or *CREB* KD, respectively (Fig. 5e). However, when the levels of mature miR-455-5p were analysed, an increase in the mature form was seen in the SB2 *ADAR1* KD and a decrease was observed in the C8161 *CREB* KD cells when compared with the NT controls, suggesting that ADAR1-mediated RNA editing may affect miR-455 biogenesis or that ADAR1 could act in an RNA-editing-independent role to affect its biogenesis (Fig. 5f). Therefore we next evaluated binding of two members of the RNase III family, Droscha and Dicer, to miR-455. Indeed, the amount of miR-455 bound to Droscha and Dicer inversely correlated with ADAR1 expression (Supplementary Fig. 5). Silencing *ADAR1* in SB2 melanoma cells induces the binding of Dicer to pre-miR-455 (the precursor stem-loop that is processed to miR-455), whereas overexpressing *ADAR1* in C8161 reduces the amount of pre-miR-455 bound to Dicer (Supplementary Fig. 5A,B respectively). Pri-miR-455 expression after pulldown of Droscha demonstrated similar results (Supplementary Fig. 5C,D). We concluded that ADAR1 reduces the ability of pri-miR-455 to bind to Droscha and be processed to mature miR-455-5p.

The function of miRNA-455 is altered after A-to-I RNA editing

To compare the functions of WT and edited (ED) miR-455, we created a set of lentiviral expression vectors overexpressing either WT miR-455, miR-455 edited at site 1 only (ED1 miR-455), miR-455 edited at site 2 only (ED2 miR-455) or miR-455 edited at both sites 1 and 2 (DED miR-455) as well as an antagomir to silence miR-455 (anti-miR-455). These vectors were then transduced into *ADAR1* KD SB2 cells, and rtPCR was carried out to confirm that the expression of the experimentally manipulated miR-455 caused changes in miR-455-5p expression (Supplementary Fig. 6A). RNA was isolated and submitted for cDNA gene expression profiling to identify potential miR-455-5p targets. TargetScan was then used to identify the genes in the WT overexpressing group that had potential miR-455-5p binding sites in their 3'-untranslated region (3'UTR). The two data sets were crossed. One of the genes that was downregulated in the WT group, with two miR-455-5p binding sites in its 3'UTR, was *CPEB1*. The main function of *CPEB1* is to activate dormant mRNAs by polyadenylating them^{26,27}. rtPCR and western blotting were used to assess *CPEB1* expression in C8161 *ADAR1* OE and SB2 *ADAR1* KD cells (Fig. 6a,b). When *ADAR1* was overexpressed in C8161 cells (leading to increased ED miR-455 and less WT miR-455), *CPEB1* expression was increased twofold at the mRNA level and 1.5-fold at the protein level, whereas when *ADAR1* was silenced in SB2 cells (leading to increased WT miR-455), *CPEB1* expression was decreased by about 70% at the mRNA level and 80% at the protein level, confirming that ADAR1 affects *CPEB1* expression (Fig. 6a,b).

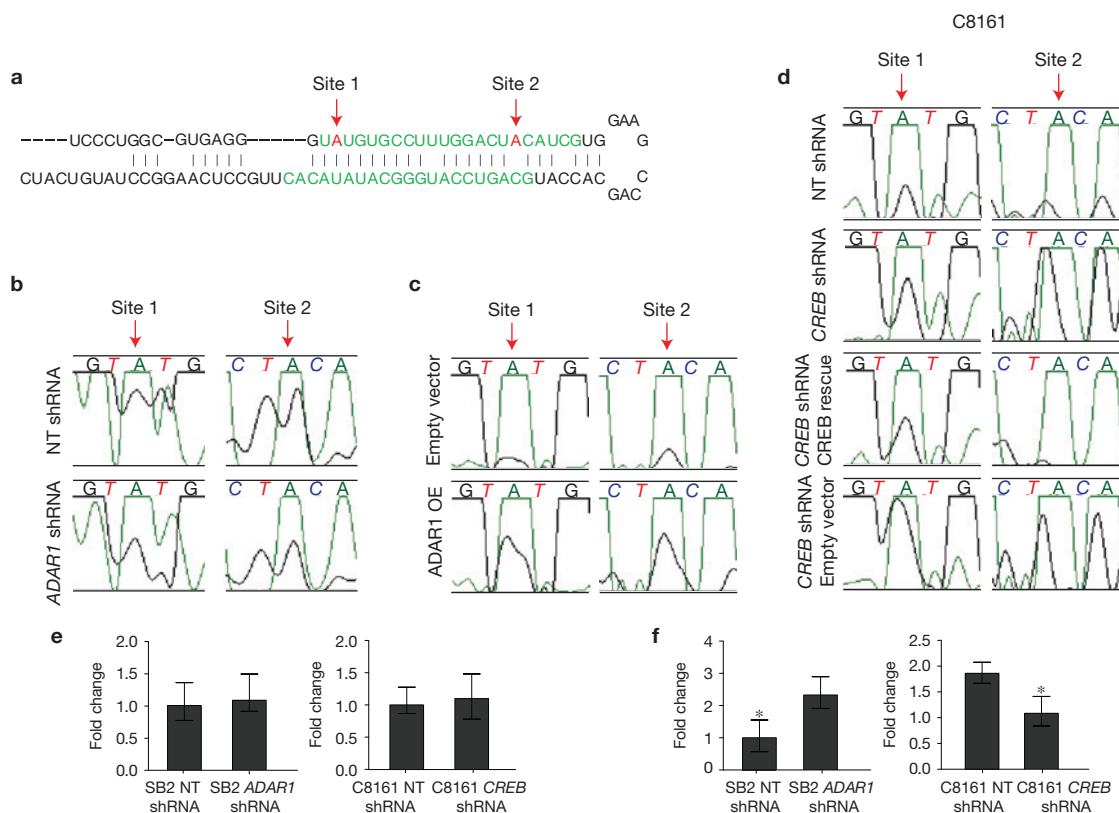


Figure 5 miR-455-5p is edited by ADAR1 at two A-to-I RNA-editing sites. **(a)** miR-455-5p with mature miRNA sequence highlighted in green. The red arrows indicate the RNA-editing sites. **(b)** RNA sequencing data indicate a decrease in A-to-I editing in SB2 cells after *ADAR1* silencing. **(c)** An increase in RNA editing is observed in C8161 cells when *ADAR1* is overexpressed. **(d)** A-to-I editing is increased on *CREB* silencing and is returned to NT levels on rescue of *CREB* expression in C8161 cells. In **b–d** the green peak represents adenosine and the black peak represents guanosine. **(e)** The

pri-miR-455 expression is not changed after *ADAR1* silencing in SB2 cells (left panel) or *CREB* silencing in C8161 cells (right panel). **(f)** Silencing *ADAR1* in SB2 cells results in increased mature miR-455-5p expression (left panel), whereas silencing *CREB* in C8161 cells causes a decrease in mature miR-455-5p expression (right panel), * $P < 0.01$. Data in **e** and **f** are the means of $n = 3$ biological independent samples. Statistical significance for **e** and **f** was determined by a two-tailed Student *t*-test; error bars represent s.d.

Next, we determined whether WT miR-455 is responsible for the change in *CPEB1* expression. Indeed, when WT miR-455 was overexpressed *CPEB1* expression was decreased 1.7-fold, whereas when any of the edited constructs were overexpressed *CPEB1* expression was increased at least twofold when compared with the empty vector control (Fig. 6c). Furthermore, when miR-455 was silenced, we found about a twofold increase in *CPEB1* expression when compared with the NT control (Fig. 6c, right two columns).

To show that *CPEB1* regulation is specific to miR-455-5p and not to miR-455-3p, we carried out a transient transfection with miR-455-5p WT, miR-455-5p DED and miR-455-3p of both C8161 and SB2 parental cells. Results clearly show that, in C8161, *CPEB1* was downregulated by ~60% when miR-455-5p WT was transfected into the cells, but not with the edited form or miR-455-3p (Fig. 6d). In SB2 we observed a significantly greater downregulation of *CPEB1* by miR-455-5p when compared with miR-455-3p and DED (Fig. 6e). Taken together, these data demonstrate that miR-455-5p is biologically active and is involved in *CPEB1* gene regulation.

We next cloned the 3'UTR of *CPEB1* into the pmir luciferase reporter construct, transfected it into manipulated miR-455 *ADAR1* KD SB2 cells, and measured luciferase activity 48 h later. Luciferase

expression was significantly decreased when miR-455 WT was overexpressed and significantly increased when anti-miR-455 was expressed when compared with the empty vector control. Moreover, when any of the three edited miR-455s were overexpressed, levels were similar to those in the empty vector control, indicating that these edited miR-455s were unable to bind to the 3'UTR and suppress *CPEB1* (Fig. 6f). To confirm these findings, the two miR-455-5p binding sites within the *CPEB1* 3'UTR (mut1 *CPEB1*, mut2 *CPEB1* and dmut *CPEB1*) were mutated to assess the binding of miR-455-5p and luciferase expression. Luciferase expression in WT miR-455 cells was similar to that in the empty vector control in all three mutated versions of *CPEB1* (Fig. 6g). Taken together, these data confirm that WT miR-455-5p can suppress *CPEB1* expression, but the edited version cannot. Thus, the effect of the unedited miR-455-5p is mediated by its sequence-dependent ability to target *CPEB1*. To further confirm the role of *CPEB1* as a tumour suppressor, we next rescued the expression of *CPEB1* in SB2 *ADAR1* KD cells. Rescue of *CPEB1* in these cells reduced their ability to invade through Matrigel coated filters, without affecting their proliferation rate (Supplementary Fig. 6B,C). Further analysis to determine potential binding sites for the edited miR-455-5p in the 3'UTR of the targets was carried

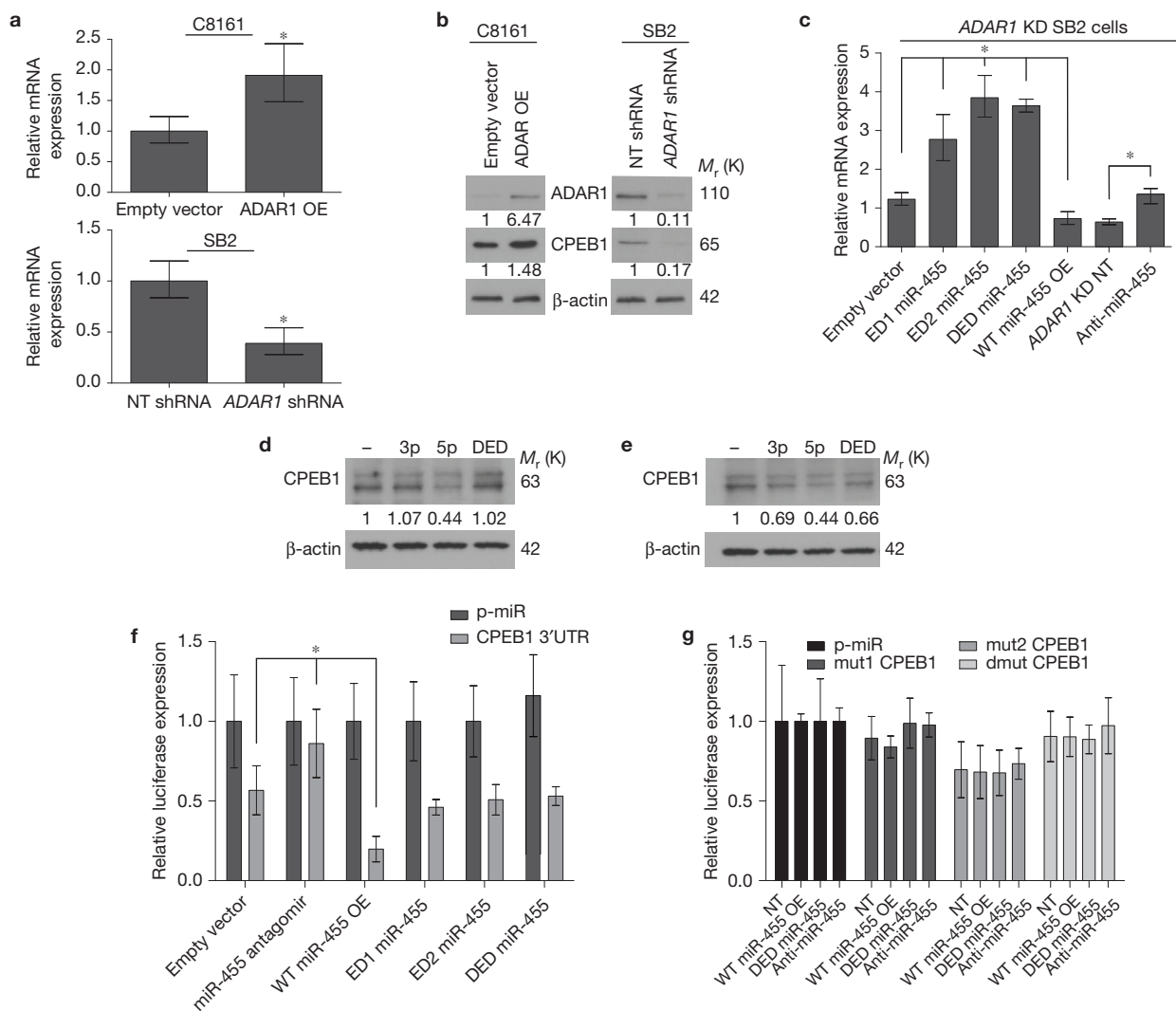


Figure 6 miR-455-5p regulates CPEB1 expression. (a) rtPCR analysis of the mRNA levels of CPEB1. Overexpression of *ADAR1* in C8161 cells resulted in increased CPEB1 expression (top panel). Silencing *ADAR1* in SB2 cells resulted in decreased CPEB1 expression (bottom panel), * $P < 0.05$ ($n = 3$ RNA samples per group, biologically independent experiments). Statistical significance by two-tailed Student *t*-test; error bars represent s.d. (b) Western blot analysis of CPEB1 expression. A 1.5-fold increase in CPEB1 protein expression was observed in C8161 *ADAR1* OE cells, whereas a reduction of about 80% was seen in SB2 *ADAR1* KD cells (data are representative of three biologically independent experiments). (c) rtPCR analysis of CPEB1 expression after miR-455 manipulation. On overexpression of WT miR-455 a significant decrease in CPEB1 was observed, whereas expression of any of the three edited forms of miR-455 led to a significant increase of CPEB1 expression, * $P < 0.05$. Silencing miR-455 resulted in increased CPEB1 expression, * $P < 0.05$. $n = 3$ RNA samples per group, biologically independent. Statistical significance by two-tailed Student *t*-test; error bars represent s.d. (d) Western blot analysis demonstrating a direct and specific

binding of miR-455-5p but not miR-455-3p or miR-455-5p DED to the 3'UTR of *CPEB1* in C8161 metastatic melanoma cells. CPEB1 is downregulated by ~60% by miR-455-5p and not by the edited form or miR-455-3p (data are representative of three biologically independent experiments). (e) In SB2 cells, a significantly stronger downregulation of CPEB1 was observed after transfection with miR-455-5p WT when compared with miR-455-5p DED or miR-455-3p (data are representative of three biologically independent experiments). (f) Luciferase expression increases on expression of anti-miR-455-5p, and decreases when WT miR-455-5p is overexpressed, * $P < 0.01$. No change was observed when the edited miR-455-5p was overexpressed, as compared with control ($n = 3$ biologically independent samples). (g) Luciferase activity of the mutational analysis of the two miR-455-5p binding sites in the 3'UTR of *CPEB1*. No significant differences were observed between any of the experimental groups ($n = 3$ biologically independent samples). Statistical significance by two-tailed Student *t*-test, error bars represent s.d. for **f** and **g**. Uncropped images of blots in **b**, **d** and **e** are shown in Supplementary Fig. 8.

out. Three genes that had potential binding sites, *RHOC*, *MDM4* and integrin $\alpha 2$, were identified, all of which have known tumour-promoting functions (Supplementary Fig. 7), which suggests that different sets of genes are regulated by the edited versus the WT form of miR-455-5p.

miR-455 contributes to melanoma tumour growth and metastasis

To elucidate the role of miR-455 in melanoma growth *in vivo*, SB2 and C8161 cells (empty vector, WT miR-455, DED miR-455 and anti-miR-455) were injected subcutaneously into nude mice. A significant

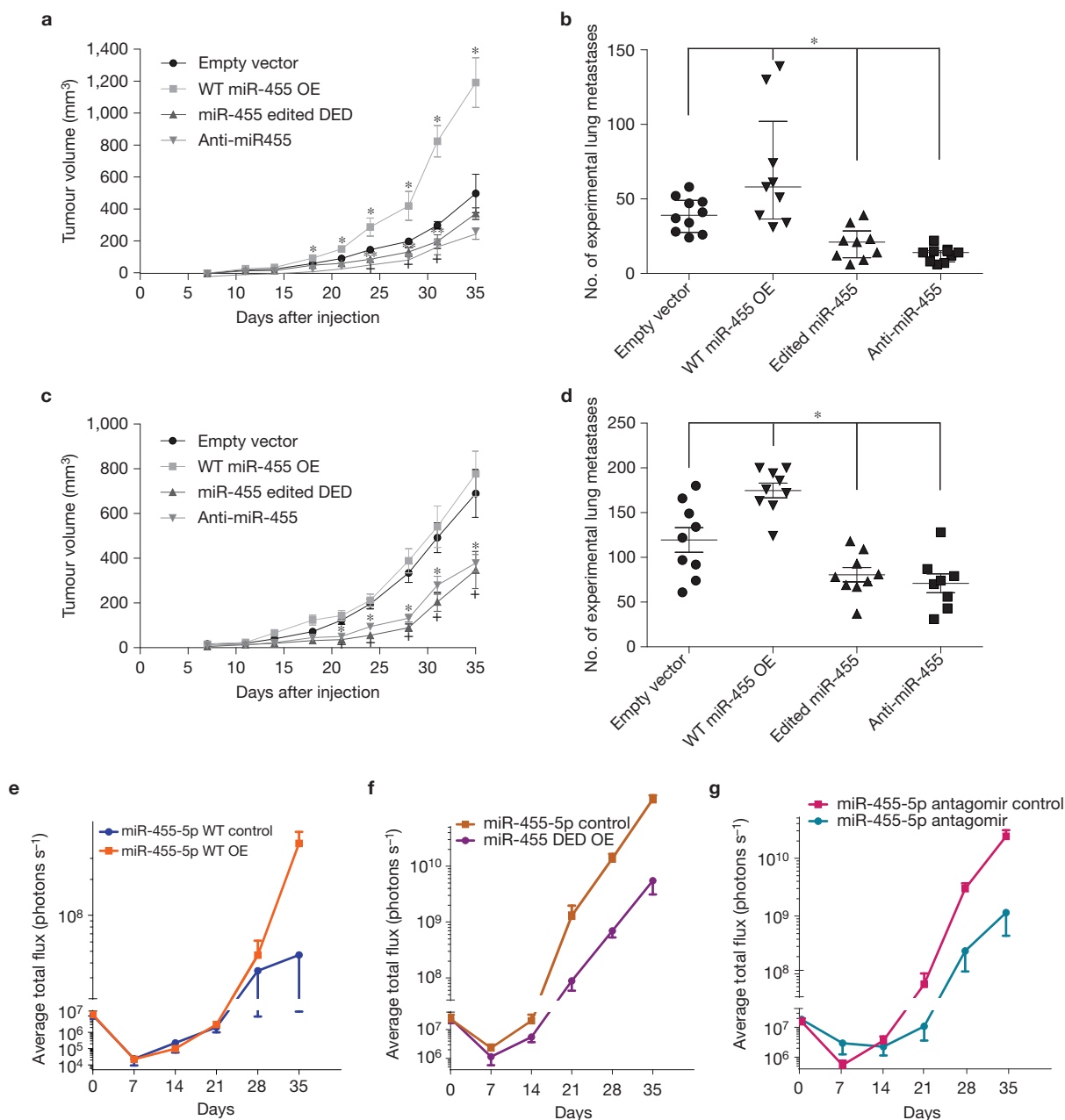


Figure 7 miR-455 overexpression leads to increased melanoma tumour growth and metastasis. **(a)** Effect of manipulation of miR-455 on subcutaneous tumour growth in SB2 cells. Overexpression of WT miR-455 results in a significant increase in tumour growth as compared with empty vector control, $*P < 0.001$, whereas silencing miR-455 or overexpressing the double-edited form of miR-455 led to a significant decrease in tumour growth, + or **, respectively, $P < 0.05$. For each group $n = 10$ mice, statistical significance by two-tailed Student t -test, $*P < 0.001$, + $P < 0.05$, and ** $P < 0.05$; error bars represent s.d. **(b)** Effect of miR-455 manipulation in SB2 cells on metastatic potential. Overexpression of WT miR-455 led to a significant increase in the number of experimental lung metastases, whereas silencing miR-455 or overexpressing the edited form of miR-455 resulted in decreased lung metastases, $*P < 0.05$. Empty vector group, $n = 10$ mice; WT miR-455 OE, edited miR-455 and anti-miR-455, $n = 9$ mice per group. Statistical significance by two-tailed Student t -test; error bars represent s.d. **(c)** Overexpression of WT miR-455 did not result in a significant increase in the already highly tumorigenic C8161 cells. Silencing miR-455 or overexpressing the edited form of miR-455 led to a significant

decrease in tumour growth, * or +, respectively, $P < 0.01$. Each group, $n = 10$ mice. Statistical significance by two-tailed Student t -test; error bars represent s.d. **(d)** Overexpression of WT miR-455 led to a significant increase in the number of experimental lung metastases in C8161 cells, whereas silencing miR-455 or overexpressing the edited form of miR-455 resulted in decreased lung metastases, $*P < 0.05$. Empty vector, WT miR-455 OE and miR-455 edited DED, $n = 9$ mice in each group; anti-miR-455, $n = 8$ mice per group. Statistical significance by two-tailed Student t -test; error bars represent s.d. **(e–g)** SB2 or C8161 luciferase labelled cells were injected intravenously, and 3 days later the mice were injected intravenously with miR-455-5p and double edited or antagonist encapsulated in 1,2-dioleoyl-sn-glycero-3-phosphocholine (DOPC) particles. **(e)** Delivery of miR-455-5p WT to mice harbouring SB2 cells increased their metastatic potential ($P = 0.0163$). **(f, g)** Delivery of double-edited miR-455-5p to mice harbouring C8161 cells decreased their metastatic potential ($P = 0.0001$) **(f)**, as did the antagonist of miR-455-5p ($P = 0.0203$) **(g)**. Each group **(d, f and g)**, $n = 6$ mice. Statistical analyses by two-way ANOVA, error bars represent s.e.m.

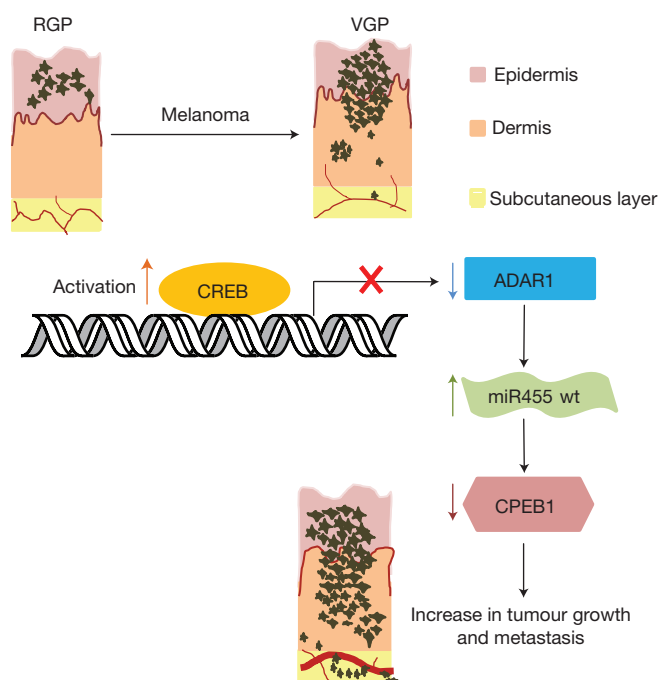


Figure 8 Model of ADAR1 RNA editing in melanoma progression. Overall model of the study showing the mechanistic understanding of how a loss of CREB-mediated ADAR1 in metastatic melanoma cells causes a shift towards the accumulation of WT miR-455-5p, thus contributing to melanoma growth and metastasis. CREB is activated in the transition from the radial growth phase (RGP) to the vertical growth phase (VGP). Activation of CREB leads to downregulation of ADAR1 in metastatic melanoma cells. Subsequently, miR-455-5p is edited in the non-metastatic melanoma cells. WT miR-455-5p preferentially binds to the 3'UTR of *CPEB1* and suppresses its expression, thus contributing to melanoma growth and metastasis.

increase in tumour growth was observed in mice injected with WT miR-455 SB2 cells but not in mice injected with C8161 cells (Fig. 7a,c). In contrast, injection of cells with either the DED miR-455 or anti-miR-455 resulted in a significant decrease in tumour growth in mice injected with SB2 cells and in mice injected with C8161 cells when compared with control cells (Fig. 7a,c). Furthermore, in mice injected with SB2 cells and in mice injected with C8161 cells, WT miR-455 overexpression led to increased incidence of experimental lung metastasis when compared with EV controls. Overexpression of either DED miR-455 or anti-miR-455 led to a significant decrease in lung metastasis in mice injected with either cell type (Fig. 7b,d). Taken together, these data show that overexpression of WT miR-455 results in increased tumour growth and incidence of lung metastasis, whereas overexpression of the edited form of miR-455 results in diminished tumour growth and lung metastasis.

To further study the specific role of miR-455-5p in melanoma metastasis, luciferase-labelled SB2 and C8161 were injected intravenously into nude mice. Three days later the mice were systemically treated with nanoliposomes carrying different miR-455-5p sequences. SB2 cells were treated with miR-455-5p WT and C8161 cells were treated with miR-455-5p WT antagonist and miR-455-5p DED. miR-455-5p WT delivery resulted in an increased ability of SB2 cells to form lung metastasis (Fig. 7e). In contrast, systemic delivery of miR-455-5p DED caused a reduction in lung metastases of C8161

cells, as did the delivery of antagonist to miR-455-5p (Fig. 7f,g). Collectively, these results demonstrate that WT miR-455-5p has an opposite effect on melanoma experimental metastasis to the edited form, and that miR-455-5p is biologically active in melanoma cells.

DISCUSSION

We have previously reported that loss of ADAR1 in melanoma contributes to melanoma growth by modulating the processing of several miRNAs independent of its RNA editing²⁴. Herein, we extended these observations to demonstrate that loss of ADAR1 in metastatic melanoma cells causes reduced A-to-I miRNA editing, leading to changes in mRNA selection. Taken together, we propose that ADAR1 contributes to the melanoma metastatic phenotype by RNA-editing-dependent and independent mechanisms.

Here, we identified RNA editing in three miRNAs: miR-324-5p, miR-378-3p, and miR-455-5p. Two ADAR1-mediated RNA-editing sites were identified in miR-455-5p, one at mature position 2 and one at mature position 17. The editing site for ADAR2 was identified in ref. 25 at position 17 in miR-455-5p in glioblastoma cell lines; our data confirm this finding and reveal an extra editing site in melanoma cells.

ADAR1-mediated RNA editing of miRNA has been shown to affect the biogenesis of miRNAs or their binding targets^{19,28}. When the mature sequence was analysed, we observed an increase in miR-455-5p WT when ADAR1 was silenced and a decrease in miR-455-5p WT when CREB was silenced. One possible explanation for these changes was detailed in a recent study, showing that ADAR1 forms a complex with Dicer to regulate miRNA processing and/or its gene silencing abilities²⁹. Therefore, loss of ADAR1 expression could lead to abnormal miRNA processing or functioning, and changes in total mature levels of miR-455-5p. Another explanation is that the edited form of miR-455-5p is not recognized or cleaved by either Dicer or Drosha for processing, as was previously shown with miR-151 and miR-142, respectively^{28,30}. We found that the amount of miR-455 bound to Dicer and Drosha was inversely correlated with ADAR1 expression.

The importance of RNA editing in melanoma growth and metastasis were verified by assessing tumour growth and metastatic capabilities after overexpression or silencing of the WT and overexpression of the edited form of miR-455. Indeed, systemic delivery of miR-455-5p WT, its edited form and antagonist *in vivo* by means of nanoparticles validated our observations and clearly demonstrated that miR-455-5p is biologically active in melanoma cells.

Using a cDNA microarray and ingenuity pathway analysis, we identified 30 known tumour suppressor genes that were downregulated when WT miR-455-5p was overexpressed. Predicted targets for miR-455-5p from TargetScan identified six genes as potential targets for miR-455-5p, and three of them (*CPEB1*, *JDP2* and *VCAN*) were on the list of known tumour suppressors (Supplementary Table 2). *CPEB1* acts as a tumour suppressor in several cancers, including gastric and thyroid KO cancer^{31,32}. When ADAR1 was overexpressed, *CPEB1* levels also increased, presumably owing to decreased WT miR-455-5p. Moreover, *CPEB1* is regulated by miR-455-5p and not by miR-455-3p. On the other hand, the edited form of miR-455-5p targets oncogenes such as *ITGA2*, *MDM4* and *RhoC*.

In summary, herein we provide evidence of CREB-mediated hypoxia expression of ADAR1 in metastatic melanoma. This loss of ADAR1 resulted in differential A-to-I RNA editing in melanoma cell lines,

particularly in miR-455-5p. In this model (Fig. 8), activation of CREB in metastatic melanoma cells leads to downregulation of ADAR1 expression. Subsequently, there is an accumulation of WT miR-455-5p in metastatic cells and more of the edited form in the non-metastatic cells. WT miR-455-5p contributes to melanoma growth and metastasis through downregulation of the tumour suppressor gene *CPEB1*. At this stage, however, the clinical relevance of this editing pathway in human melanoma is yet to be determined. □

METHODS

Methods and any associated references are available in the [online version of the paper](#).

Note: Supplementary Information is available in the online version of the paper

ACKNOWLEDGEMENTS

We thank S. Maas from NIH for providing the ADAR1 A-to-I RNA-editing hairpin loop luciferase reporter plasmid. We thank W. Choi for her help with the miRNA microarray. We thank R. Rajesha for his technical help and support. These studies are supported by SINE, an MDACC grant and NIH Skin Cancer SPORE p50 CA093459.

AUTHOR CONTRIBUTIONS

M.B.-E. conceived and supervised the project. E.S. and A.K.M. designed and carried out experiments and analysed most of the data. R.R.B., T.K., L.H., M.E.V., G.V.-T. and A.S. carried out experiments and analysed data. H.J.L., S.J.K. and I.J.F. helped with the spontaneous animal model. C.I., A.G.R., K.M.N., K.Z., D.B., S.J.M.J., I.B., M.M., Y.-y.W., A.K.E., P.H. and J.E.G. carried out sequencing and analysis. A.K.S., G.A.C. and G.M. helped with miRNA analysis.

COMPETING FINANCIAL INTERESTS

The authors declare no competing financial interests.

Published online at www.nature.com/doi/10.1038/ncb3110

Reprints and permissions information is available online at www.nature.com/reprints

- Siegel, R., Ma, J., Zou, Z. & Jemal, A. Cancer statistics, 2014. *CA Cancer J. Clin.* **64**, 9–29 (2014).
- Miller, A. J. & Mihm, M. C. Jr Melanoma. *N. Engl. J. Med.* **355**, 51–65 (2006).
- Xie, S. *et al.* Dominant-negative CREB inhibits tumor growth and metastasis of human melanoma cells. *Oncogene* **15**, 2069–2075 (1997).
- Mobley, A. K., Braeuer, R. R., Kamiya, T., Shoshan, E. & Bar-Eli, M. Driving transcriptional regulators in melanoma metastasis. *Cancer Metastasis Rev.* **31**, 621–632 (2012).
- Jean, D., Harbison, M., McConkey, D. J., Ronai, Z. & Bar-Eli, M. CREB and its associated proteins act as survival factors for human melanoma cells. *J. Biol. Chem.* **273**, 24884–24890 (1998).
- Melnikova, V. O. & Bar-Eli, M. Transcriptional control of the melanoma malignant phenotype. *Cancer Biol. Ther.* **7**, 997–1003 (2008).
- Melnikova, V. O., Mourad-Zeidan, A. A., Lev, D. C. & Bar-Eli, M. Platelet-activating factor mediates MMP-2 expression and activation via phosphorylation of cAMP-response element-binding protein and contributes to melanoma metastasis. *J. Biol. Chem.* **281**, 2911–2922 (2006).
- Dobroff, A. S. *et al.* Silencing cAMP-response element-binding protein (CREB) identifies CYR61 as a tumor suppressor gene in melanoma. *J. Biol. Chem.* **284**, 26194–26206 (2009).
- Bertolotto, C. *et al.* Microphthalmia gene product as a signal transducer in cAMP-induced differentiation of melanocytes. *J. Cell Biol.* **142**, 827–835 (1998).
- Melnikova, V. O. *et al.* CREB inhibits AP-2 α expression to regulate the malignant phenotype of melanoma. *PLoS ONE* **5**, e12452 (2010).
- Venables, J. P. Unbalanced alternative splicing and its significance in cancer. *Bioessays* **28**, 378–386 (2006).
- David, C. J. & Manley, J. L. Alternative pre-mRNA splicing regulation in cancer: pathways and programs unhinged. *Genes Dev.* **24**, 2343–2364 (2010).
- Gallo, A. & Galardi, S. A-to-I RNA editing and cancer: from pathology to basic science. *RNA Biol.* **5**, 135–139 (2008).
- Levanon, E. Y. *et al.* Systematic identification of abundant A-to-I editing sites in the human transcriptome. *Nat. Biotechnol.* **22**, 1001–1005 (2004).
- Laurencikiene, J., Kallman, A. M., Fong, N., Bentley, D. L. & Ohman, M. RNA editing and alternative splicing: the importance of co-transcriptional coordination. *EMBO Rep.* **7**, 303–307 (2006).
- Jin, Y., Zhang, W. & Li, Q. Origins and evolution of ADAR-mediated RNA editing. *JUBMB Life* **61**, 572–578 (2009).
- Bass, B. L. RNA editing by adenosine deaminases that act on RNA. *Annu. Rev. Biochem.* **71**, 817–846 (2002).
- Keegan, L. P., Gallo, A. & O'Connell, M. A. The many roles of an RNA editor. *Nat. Rev. Genet.* **2**, 869–878 (2001).
- Maas, S., Rich, A. & Nishikura, K. A-to-I RNA editing: recent news and residual mysteries. *J. Biol. Chem.* **278**, 1391–1394 (2003).
- Hood, J. L. & Emeson, R. B. Editing of neurotransmitter receptor and ion channel RNAs in the nervous system. *Curr. Top. Microbiol. Immunol.* **353**, 61–90 (2012).
- Wulff, B. E. & Nishikura, K. Modulation of microRNA expression and function by ADARs. *Curr. Top. Microbiol. Immunol.* **353**, 91–109 (2012).
- Zinshteyn, B. & Nishikura, K. Adenosine-to-inosine RNA editing. *Wiley Interdiscip. Rev. Syst. Biol. Med.* **1**, 202–209 (2009).
- Heale, B. S. *et al.* Editing independent effects of ADARs on the miRNA/siRNA pathways. *EMBO J.* **28**, 3145–3156 (2009).
- Nemlich, Y. *et al.* MicroRNA-mediated loss of ADAR1 in metastatic melanoma promotes tumor growth. *J. Clin. Invest.* **123**, 2703–2718 (2013).
- Alon, S. *et al.* Systematic identification of edited microRNAs in the human brain. *Genome Res.* **22**, 1533–1540 (2012).
- Si, K. *et al.* A neuronal isoform of CPEB regulates local protein synthesis and stabilizes synapse-specific long-term facilitation in aplysia. *Cell* **115**, 893–904 (2003).
- Sasayama, T. *et al.* Over-expression of Aurora-A targets cytoplasmic polyadenylation element binding protein and promotes mRNA polyadenylation of Cdk1 and cyclin B1. *Genes Cells* **10**, 627–638 (2005).
- Kawahara, Y., Zinshteyn, B., Chendrimada, T. P., Shiekhattar, R. & Nishikura, K. RNA editing of the microRNA-151 precursor blocks cleavage by the Dicer-TRBP complex. *EMBO Rep.* **8**, 763–769 (2007).
- Ota, H. *et al.* ADAR1 forms a complex with Dicer to promote MicroRNA processing and RNA-induced gene silencing. *Cell* **153**, 575–589 (2013).
- Yang, W. *et al.* Modulation of microRNA processing and expression through RNA editing by ADAR deaminases. *Nat. Struct. Mol. Biol.* **13**, 13–21 (2006).
- Caldeira, J. *et al.* *CPEB1*, a novel gene silenced in gastric cancer: a *Drosophila* approach. *Gut* **61**, 1115–1123 (2012).
- Zhang, J. H. *et al.* Cytoplasmic polyadenylation element binding protein is a conserved target of tumor suppressor HRPT2/CDC73. *Cell Death Differ.* **17**, 1551–1565 (2010).
- Levanon, E. Y. *et al.* Evolutionarily conserved human targets of adenosine to inosine RNA editing. *Nucleic Acids Res.* **33**, 1162–1168 (2005).
- Galeano, F. *et al.* Human BLCAP transcript: new editing events in normal and cancerous tissues. *Int. J. Cancer* **127**, 127–137 (2010).

METHODS

Cell lines and culture conditions. All of the human melanoma cell lines used in our studies were maintained in MEM supplemented with 2 mM glutamine, 1% non-essential amino acids and 10% fetal bovine serum (FBS). The 293FT cells (Invitrogen) used to produce the lentiviral shRNA were maintained in DMEM supplemented with 10% FBS according to the manufacturer's instructions. All cell lines used in our studies were tested before their usage for authentication by DNA fingerprinting using the short tandem repeat method.

Lentiviral shRNA. *CREB*-targeting shRNA (target sequence 5'-GAGAGAGGTCCGTCTAATG-3'), *ADAR1*-targeting shRNA (target sequence 5'-CTTCTGTGAGA-3') and a non-targeting shRNA (NT shRNA, target sequence 5'-TTCTCCGAACGTGTCACGT-3') were designed with a hairpin, inserted into the pSIH lentiviral vectors and transfected into 293FT (human embryonic kidney) cells to generate lentiviral particles. The lentivirus system and cell transduction were generated as described previously⁸. To silence *CREB*, highly metastatic C8161 and MeWo cell lines plated at 70% confluency in six-well plates were transduced with the virus. To silence *ADAR1*, SB2 cells were plated at 60% confluency in six-well plates and transduced with the virus. After 16 h, the virus-containing medium was removed and replaced with normal growth medium. Transduced cells were sorted using green fluorescent protein.

Non-targetable *CREB* expression vector. The lentiviral *CREB* expression vector was developed as described above. Briefly, total RNA was extracted from A375SM cells, and the open reading frame of *CREB* was amplified by PCR from the reverse transcription product with the following two primers: CreB-XbaI, 5'-GCTCTAGAATGACCATGGAATCTGGAGCCGAG-3'; CreB-Cla-H3R, 5'-CCCAAGCTTatcgATTAATCTGATTTGTGGCAGTAAAG-3'. To create a non-targeting *CREB* expression vector, we used the following oligonucleotides: CreB1B-ReF, 5'-GAAGCAGCACGAAAGAGAGAAGTGCAGCTGATGAAGAACAGGGAAGCAG-3'; CreB1B-ReR, 5'-CTGCTTCCCTGTTCTTCATCAGTCGCACTTCTCTCTTCTGTGCTGCTTC-3'. To rescue *CREB* expression in stably *CREB*-silenced cells, C8161 and MeWo *CREB* shRNA or NT shRNA cells were plated in six-well plates and transduced with virus containing either the non-targeting *CREB* expression vector or an empty vector. After 48 h, the cells were expanded and selected. *CREB* expression was confirmed through western blot analysis.

Western blot analysis. To detect the expression of *CREB* (rabbit monoclonal antibody no 9197L, clone 48H2, Cell Signaling), phospho-*CREB* (Ser 133 rabbit antibody no 9191s, Cell Signaling), *ADAR1* (rabbit antibody, SAB4200541, Sigma), *ADAR2* (rabbit polyclonal antibody, GTX114237, GeneTex) or *CPEB1* (rabbit antibody 13583s, Cell Signaling) we loaded 20 µg of whole-cell protein lysates on SDS-PAGE and carried out western blotting as described previously⁸. Blots were incubated with primary antibodies (1:1,000 *CREB*, phospho-*CREB*, *CPEB1*; 1:1,000 anti-*ADAR1*). Densitometry was carried out using ImageJ software (NIH). All western blot analyses were carried out in three independent experiments.

ChIP assay. ChIP assays were carried out using a ChIP-IT Express kit (Active Motif) according to the manufacturer's protocol. Briefly, cells were fixed with 1% formaldehyde, and the crosslinking reaction was stopped with 0.125 M glycine. The cells were pelleted and resuspended in a hypotonic buffer, and cell nuclei were isolated using a Dounce homogenizer. The chromatin was then sheared into 200–1,000-bp fragments by adding an enzymatic solution for 10 min at 37 °C. Fractions of the chromatin solutions were incubated overnight at 4 °C with either 3 µg of anti-*CREB* or IgG control antibodies crosslinked to magnetic beads. The immune complexes were then eluted from the magnetic beads, and proteins were reverse crosslinked at 65 °C for 2.5 h. Proteins were digested with 2 µl of proteinase K at 37 °C for 1 h, extracted in elution buffer and analysed through PCR. For binding site 1 a 151-bp fragment (primer sequences: forward, 5'-CCTTGGTCGTTTGACGAGAT-3'; reverse, 5'-GGAAAAACAAGGCACACAAAA-3'), for binding site 2 a 180-bp fragment (forward, 5'-TGCCTTTGTTTCCCTTTTGC-3'; reverse, 5'-AACTCCGGCTTCAAGAGAT-3') and for both binding sites a 317-bp fragment (forward, 5'-CCTTGGTCGTTTGACGAGAT-3'; reverse, 5'-AACTCCGGCTTCAAGAGAT-3') of the *ADAR1* promoter was amplified by PCR. For miR-455-Dicer or miR-455-Drosha co-immunoprecipitation, melanoma cells were collected with immunoprecipitation buffer (50 mM Tris-HCl (pH 7.4), 150 mM NaCl, 0.05% IGEPAL, 1 mM PMSF and proteinase inhibitor cocktail). Cells were then sonicated briefly for complete lysis and centrifuged. The supernatant was immunoprecipitated with the Dicer antibody (1:100 dilution, antibody no 14601, Abcam) overnight followed by incubation with magnetic protein G beads for 1 h. After three washes with immunoprecipitation buffer, the RNA was collected with 50 mM NaHCO₃ in 1% SDS. TRIzol reagent was used to purify the RNA. pri-miR-455 (Applied Biosystems) was used for the Drosha immunoprecipitation. All ChIP analyses were carried out in three independent experiments.

Pri-miRNA sequencing. Total RNA was extracted from cells and reverse transcription was carried out. PCR with reverse transcription was carried out to amplify the pri-miRNA sequence from 10 different samples. The PCR product was then sent to SeqWright and subjected to Sanger sequencing. On return the sequence chromatograms were analysed for editing sites. Primers used for pri-miR-455 sequencing were the following: forward, 5'-CGAGCTTCCTTCTGCAGGT-3'; reverse, 5'-CACCAGTCCATCCCACA-3'.

Reporter constructs and luciferase activity analysis. The *ADAR1* A-to-I RNA-editing hairpin loop luciferase reporter was used as described previously³⁵. The *ADAR1* promoter luciferase assay was carried out as follows. The *ADAR1* promoter region (nucleotides -1,000 to +65 from the transcription initiation site) was amplified from C8161 genomic DNA using the following primers: forward, 5'-GGGGTACCAGCCTCGGTTTCTACACCTGC-3'; reverse, 5'-CCGC TCGAGGGTTCAATTTTCGCTTTCGTTTC-3'. The fragment was digested with KpnI and XhoI and ligated into the pGL3-basic vector (Promega). Analysis of transcription factor binding sites was carried out using Genomatix software. Site-directed mutagenesis of the CRE sites, replacing CG of the GACGTCA CRE site with AT, was carried out using the QuikChange II XL site-directed mutagenesis kit (Stratagene) according to the manufacturer's instructions. The *CPEB1* 3'UTR miRNA-binding luciferase assay was carried out as follows. The 3'UTR region of *CPEB1* was amplified from C8161 genomic DNA using the following primers: forward, 5'-GGGCCAAAGCTTTCCCAAGGACAAGGAAAATG-3'; reverse, 5'-GGACTAGTCACATGGTCCCACCATTCCT-3'. The fragment was digested with HindIII and SpeI and ligated into the pmir vector (Ambion). Site-directed mutagenesis was carried out using the QuikChange II XL site-directed mutagenesis kit (Stratagene) according to the manufacturer's instructions. Transient transfections were carried out using Lipofectin or Lipofectamine 2000 (Invitrogen) according to the manufacturer's instructions. In a 24-well plate, a total of 2.5 × 10⁴ cells per well were transfected with 0.8 µg of the empty pGL3 expression vector or with 0.8 µg of the pGL3-*ADAR1* or pGL3-*ADAR1*-promoter-mutant-containing firefly luciferase expression constructs. For each transfection, 2.5 ng of cytomegalovirus-driven *Renilla* luciferase reporter construct (pRL-CMV, Promega) was included. After 4 h, the transfection medium was replaced with serum-containing growth medium. After 48 h, the cells were harvested and lysed, and the luciferase activity was assayed using a Dual-Luciferase reporter assay system (Promega) according to the manufacturer's instructions. Luciferase luminescence (relative light intensity × 10⁶) was measured with a LUMIstar microplate reader (BMG LABTECH). The ratio of firefly luciferase activity to CMV-driven *Renilla* luciferase activity was used to normalize any differences in transfection efficiency among samples. All constructs were fully sequenced in both directions before use. All luciferase analyses were carried out in three independent experiments.

BLCAP sequencing. RNA was extracted from C8161, C8161 *ADAR1* OE and normal melanocyte cells using an RNAqueous phenol-free total RNA isolation kit (Life Science Technologies). Double-stranded cDNA was made using a cDNA Synthesis System (Roche) kit using 10 µg of RNA input. PCR reactions were carried out to amplify the region on the *BLCAP* gene known to be edited (exon 2—on chromosome 20) using the primers 5'-CTCCCA TTAGTCGTTCCCT and 5'-AGCAGGTAGAAGCCCATGAA. Amplification parameters were as follows: 1 × [95 °C–3 min]; 35 × [94 °C–0.5 min, 55 °C–0.5 min, 72 °C–1 min]; 1 × [72 °C–5']. Each replicate PCR amplicon (168 nucleotides) was confirmed in a 1% agarose gel. Ion Torrent libraries were made using the Ion Plus Fragment Library Kit (Life Science Technologies), where each 100 ng PCR amplicon was prepared as an individual library by ligating to a unique Ion Xpress Barcode Adaptor (Life Science Technologies) following the manufacturer's recommendations. The barcoded libraries were amplified for five cycles, and re-qualified libraries were pooled and templated using the Ion One Touch 2 system (Life Science Technologies) and sequenced on an Ion Torrent Personal Genome Machine (Life Science Technologies) using a 318 chip v2 following the manufacturer's recommendations. Raw sequencing data were concatenated into one 'reference' file and indexed it using Burrows–Wheeler Aligner (BWA) software. We aligned the sequences to this reference file using BWA (ref. 36) and measured the allele frequency of RNA editing sites in each sample.

Animals, tumour growth and experimental metastasis. Female athymic BALB/c nude mice (National Institutes of Health, NCI, Frederick Cancer Research Institute) were housed in laminar flow cabinets under specific pathogen-free conditions and used at 8 weeks of age. The mice were maintained in facilities approved by the American Association for Accreditation of Laboratory Animal Care and in accordance with the current regulations and standards of the US Department of Agriculture, Department of Health and Human Services, National Institutes of Health and our institutional regulations. The sample size was determined to have a 80% power with 95% confidence. In accordance with the Institutional Animal

Care and Use Committee, when the largest dimension of a subcutaneous tumour reached 1.5 cm, the mice were killed in a CO₂ chamber. Subcutaneous tumours were produced by injecting 5×10^5 C8161 cells or 1×10^6 SB2 cells (single-cell suspensions, more than 95% viability by a trypan blue exclusion test) in 0.2 ml of Hanks' buffered salt solution into the right flank of each mouse. Tumour growth was recorded twice weekly with a calliper and calculated as $a \times b^2/2$ mm³ (a, long diameter; b, short diameter). Mice were euthanized when the tumour volume reached 1.5 cm³ or when ulceration appeared. Each group included 10 mice. To determine metastatic potential, 1×10^6 tumour cells, processed as described above, were injected into the tail veins of mice (0.1 ml/mouse). After 30 days for C8161 and 60 days for SB2 cells, the mice were killed and autopsied. The lungs were removed and fixed in Bouin's fixative solution, and the macroscopic surface tumour nodules were counted. Each group included seven to nine mice. Excluded mice were those that died for unknown reasons unrelated to tumour burden or lung metastasis. The experiments were not randomized. The investigators were not blinded to the group allocation during the experiments.

Spontaneous metastasis model. To determine the spontaneous metastatic potential of the cell lines, 2×10^5 cells of C8161 or 5×10^5 cells of SB2 luciferase-expressing clones in 20 μ l Ca²⁺/Mg²⁺-free Hank's balanced salt solution were injected into the skin ridge of the external ear. Mice were ear-tagged and imaged weekly through an IVIS 100 series system (Xenogen). When the tumour reached 9–10 mm in diameter, 4–5 weeks later for C8161 and 4–7 weeks later for SB2, the ear was resected, and the ear canal was reconstructed. Mice were followed up to determine the development of regional lymph node metastasis by *in vivo* imaging and autopsy. A two-way ANOVA test was used for comparison of the results (at week 4 * $P < 0.0001$).

***In vivo* imaging.** For bioluminescence imaging, mice received an intraperitoneal injection of 0.2 ml of 15 mg ml⁻¹ D-luciferin under 1–2% inhaled isoflurane anaesthesia. The bioluminescence signals were monitored using an IVIS 100 series system (Xenogen) consisting of a highly sensitive cooled charge-coupled device (CCD) camera. Living Image software (Xenogen) was used to grid the imaging data and integrated the total bioluminescence signals in each boxed region. D-luciferin potassium salt (luciferin; Gold Bio Technology), was dissolved in PBS and then filtered through a 0.22 μ m membrane for sterilization. Two kinetic bioluminescent acquisitions were collected between 0 and 20 min after D-luciferin injection to confirm the peak photon emission, recorded as the maximum photon efflux per second. Data were analysed and quantified by using the total photon flux emission (photons s⁻¹) in the regions of interest.

***In vivo* liposomal delivery experiment.** To determine whether siRNA mimics delivered by neutral liposomes could reach the experimental lung tumours, siRNA mimics were incorporated into DOPC liposomes as described previously^{37,38}. The liposomes were injected intravenously twice weekly, starting 3 days after melanoma cell injections. The following miRNA mimics were purchased from Life Technologies: human miR-455-5p WT, UAUGUGCCUUUGGACUACAUCG; customized miR-455-5p DED, UGUGCGCCUUUGGACUGCAUCG; human miR-455 inhibitor—antagomir (catalogue no 4464088, Life Technologies); miRNA mimic inhibitor negative control (catalogue no 4464079, Life Technologies); miRNA mimic negative control (catalogue no 4464060, Life Technologies). Statistical significance by two-way ANOVA; s.e.m.

Delivery of miRNA-455 mimics *in vitro*. The mimics of miRNA-455 were delivered into two cell lines (C8161, and SB2 parental) by using Lipofectamine RNAiMAX following the manufacturer's instruction. 25 pmol of miR-455 mimics were used for 0.7×10^6 cells in six-well plates. Cells were collected 24 h after transfection for relevant analyses for western blot and rtPCR. The following mimic sequences of miRNA-455 were purchased from Life Technologies: human miR-455-5p, UAUGUGCCUUUGGACUACAUCG; human miR-455-3p, GCAGUCCAUGGGCAUAUACAC; customized miR-455-5p DED, UGUGCGCCUUUGGACUGCAUCG; miRNA mimic negative control (catalogue no 4464060, Life Technologies).

Expression profiling studies. Total RNA was isolated from C8161 CREB shRNA or NT shRNA (for miRNA array) or from SB2 cells overexpressing WT or edited miR-455-transduced melanoma cells using the mirVana RNA isolation kit (Ambion). RNA quality was assessed using an RNA bioanalyser chip (Agilent). For the cDNA microarray, RNA was submitted to Phalanx Biotech Group for expression profiling and analysis. Gene expression analysis was carried out between the two samples. For the miRNA array, the TaqMan Array Human MicroRNA Card Set v3.0 was used.

Matrigel invasion assay. Matrigel invasion assays were carried out using Biocoat Matrigel invasion chambers (BD Biosciences). Briefly, 1.5×10^4 cells diluted in 500 μ l of serum-free MEM were placed on top of the upper chamber of the Matrigel plate in triplicates. The lower chamber contained MEM supplemented with 20% FBS. Matrigel plates were incubated for 24 h at 37 °C. A Hema3 stain set was used to stain the cells that migrated to the lower surface of the Matrigel filter (Fisher Scientific). Filters were glued on a microscope slide. Pictures from different fields were taken under the microscope and the stained cells were counted and statistically analysed.

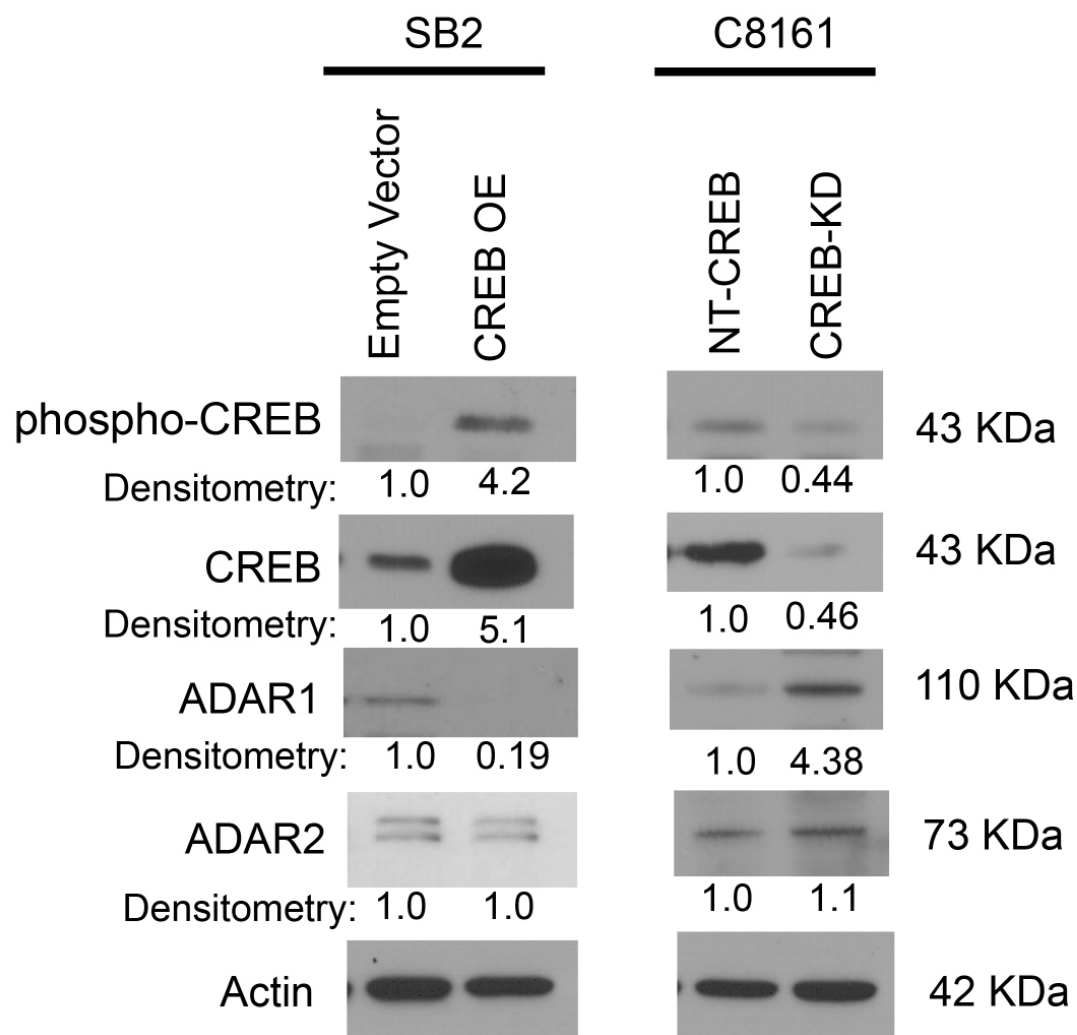
***In vitro* proliferation assay (MTT).** Five thousand cells were plated in each well of 96-well plates that were used in this experiment (12 repetitions for each sample). The cells that were plated were SB2 parental, SB2 ADAR1 KD, ADAR1 non-target control and SB2 ADAR1 KD + CPEB1 OE. The cells were cultured for 5 days in 10% FBS normal growth MEM medium. Cell growth was analysed by the colorimetric MTT (3-(4,5-dimethylthiazol-2-yl)-2,5-diphenyltetrazolium bromide) assay, which determines relative number of cells on the basis of the conversion of MTT to formazan (which has a purple colour) in viable cells. Each day after plating of the cells, MTT (Sigma) was added to each well at 1 mg ml⁻¹ concentration in PBS, 20 μ l for each well. After addition of the MTT, a 2 h incubation period was applied at 37 °C. Medium and MTT were removed from the wells and were replaced by 100 μ l of dimethylsulphoxide (Sigma). After 10 min of incubation at room temperature with dimethylsulphoxide the plate was read and quantified by measuring the absorbance at 570 nm using an Epoch BioTek plate reader. This procedure was repeated daily over 5 days to see if there were differences between the proliferation rates of cell lines that were ADAR1 and CPEB1 manipulated using lentivirus stable transduction.

Quantitative rtPCR. RNA (20 ng μ l⁻¹) from the SB2 and C8161 cell lines was harvested using a mirVana kit (Ambion) according to the manufacturer's instructions. The RNA was then transcribed into cDNA using TaqMan reverse transcriptase reagents for general cDNA or a TaqMan miRNA reverse transcription kit and miR-455-5p-specific primer for miRNA-specific cDNA (Applied Biosystems). The primers and fluorescence probes were obtained from Applied Biosystems. Reaction components for PCR with reverse transcription and amplifications have been described previously³⁸. Amplifications were run in triplicate, and averages were obtained after normalization with 18s ribosomal RNA or RNU6 (Applied Biosystems). Data were expressed as fold change.

Statistical analysis. Student's *t* test was used to evaluate the statistical significance of the *in vitro* and *in vivo* data; a two-way ANOVA test was also used with the *in vivo* data. Values for tumour growth are given as a mean volume \pm s.d., and *P* values less than 0.05 were considered statistically significant.

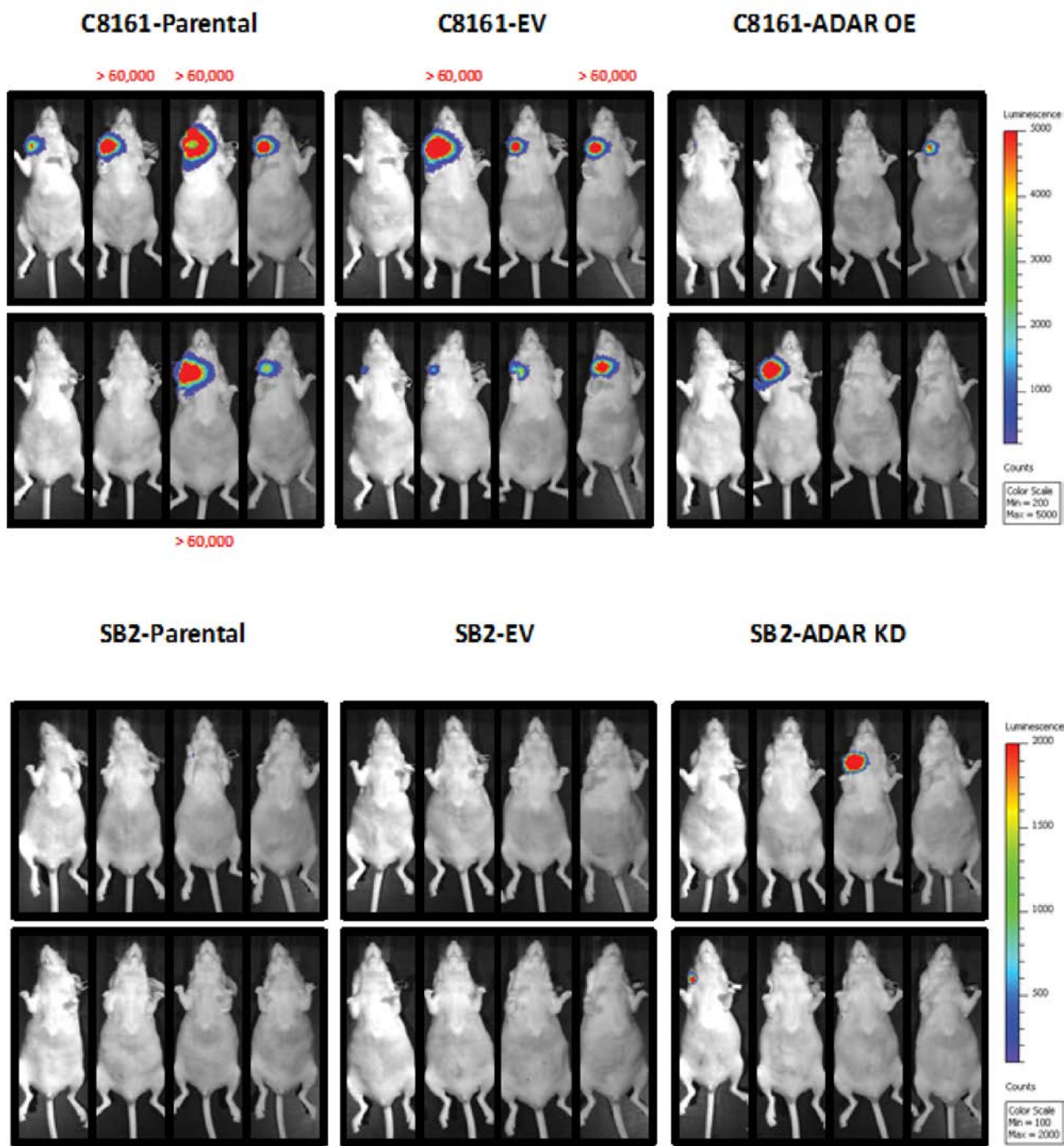
Gene Expression Omnibus accession number. Full microarray data are deposited in NCBI Gene Expression Omnibus archives (GSE31963).

35. Gommans, W. M., McCane, J., Nacarelli, G. S. & Maas, S. A mammalian reporter system for fast and quantitative detection of intracellular A-to-I RNA editing levels. *Anal. Biochem.* **399**, 230–236 (2010).
36. Li, H. & Durbin, R. Fast and accurate short read alignment with Burrows–Wheeler transform. *Bioinformatics* **25**, 1754–1760 (2009).
37. Landen, C. N. Jr *et al.* Therapeutic EphA2 gene targeting using neutral liposomal small interfering RNA delivery. *Cancer Res.* **65**, 6910–6918 (2005).
38. Villares, G. J. *et al.* Targeting melanoma growth and metastasis with systemic delivery of liposome-incorporated protease-activated receptor-1 small interfering RNA. *Cancer Res.* **68**, 9078–9086 (2008).



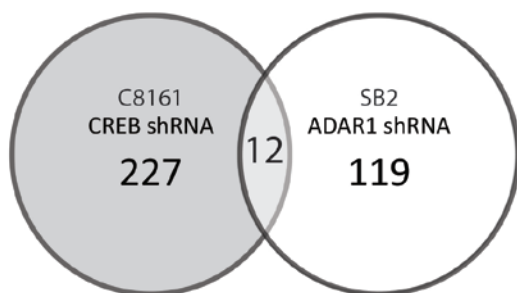
Supplementary Figure 1 ADAR2 is not regulated by CREB. Western blot analyses demonstrating that overexpression of CREB in SB2 cells and silencing CREB in C8161 cells did not affect the expression of ADAR2 in these cells. Note a doublet bands in ADAR2

expression in SB2 cells which represent two different isoforms (73,76KDa) (data are representative of 3, biologically independent experiments). Uncropped images of the blots are shown in Supplementary Figure 8.



Supplementary Figure 2 Luciferase imaging of lymph node metastasis in nude mice. Images of mice after the primary tumors were removed show the presence or absence of local lymph node metastases. These mice represent the results described in Figure 4C (n=8 mice in each group).

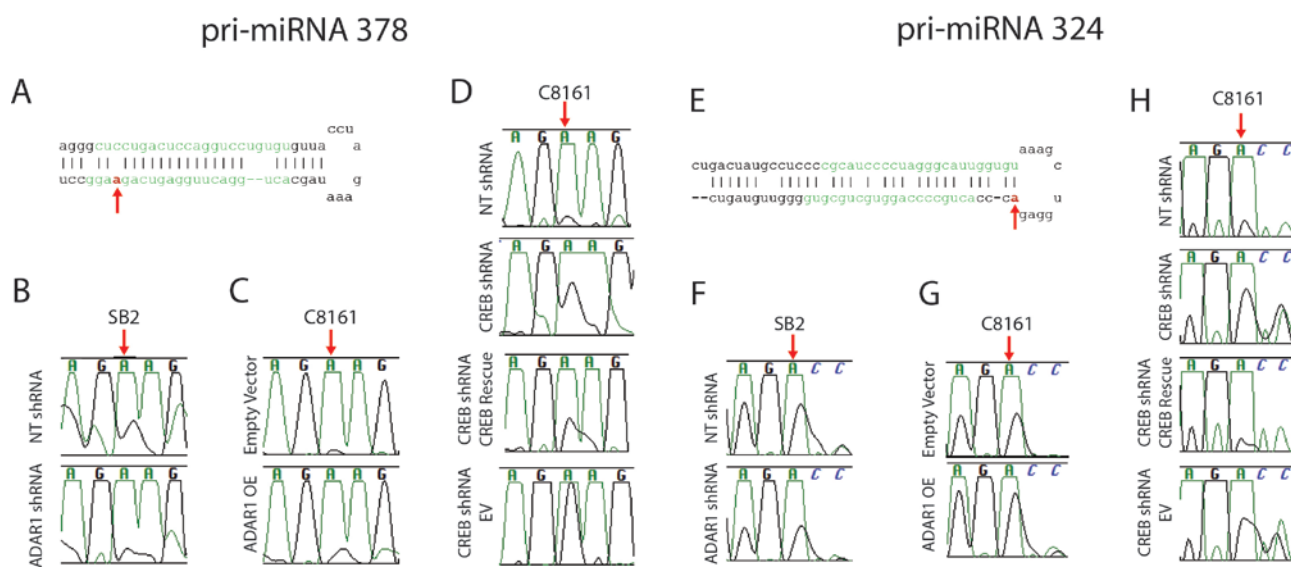
A



B

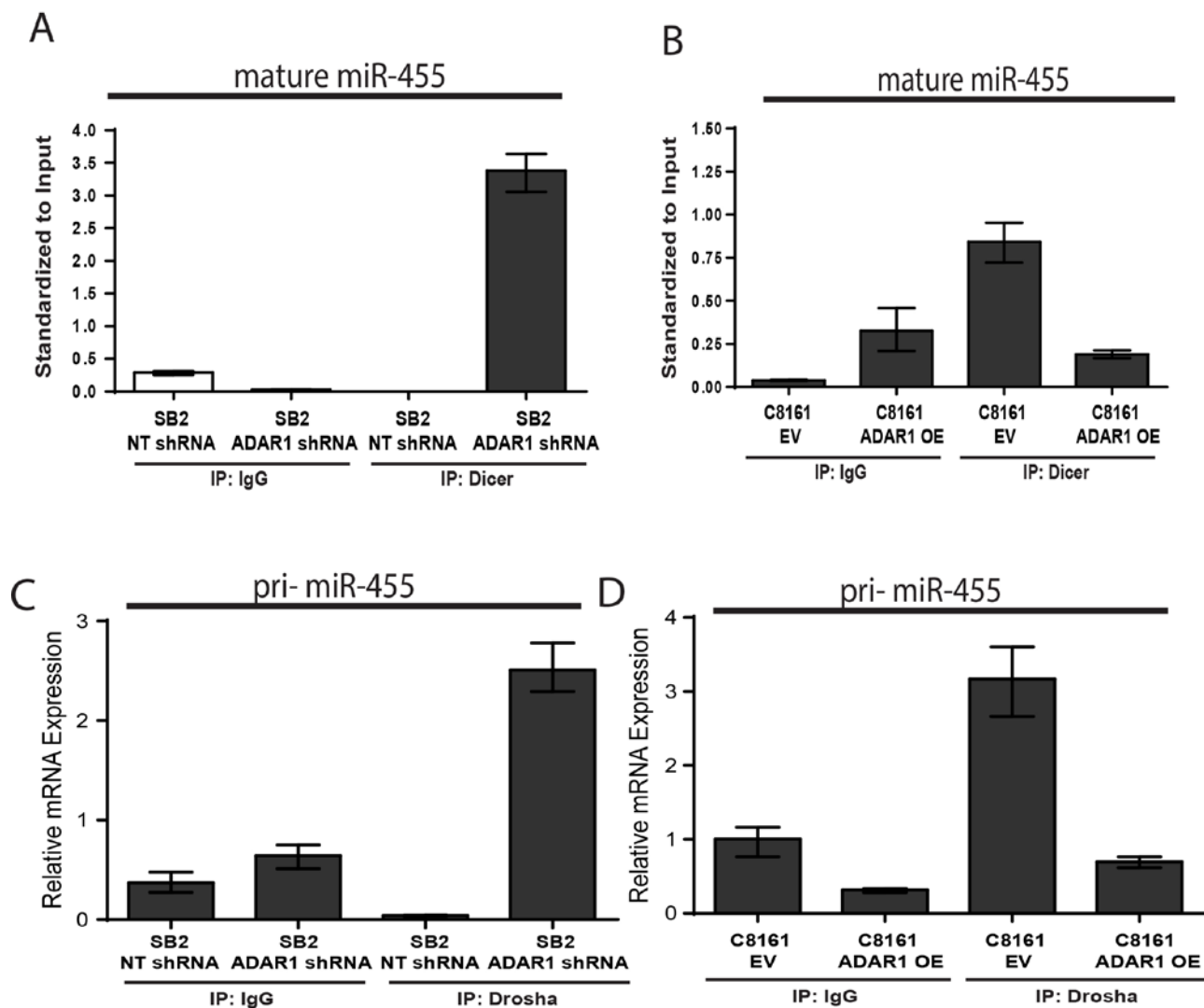
microRNA	C8161 CREB shRNA Fold Change	SB2 ADAR1 shRNA Fold Change
hsa-miR-886-3p	-7.3	8.1
hsa-miR-532-3p	-3.8	2.2
hsa-miR-378	-3.6	5.9
hsa-miR-185	-3.3	2.4
hsa-miR-151-3p	-2.9	4.2
hsa-miR-324-5p	-2.9	5.6
hsa-miR-455-5p	-2.8	4.9
hsa-miR-26a	2.1	-36.3
hsa-miR-222	2.8	-10.8
hsa-miR-523	3.9	-2.4
hsa-miR-494	4.1	-2.7
hsa-miR-130a	65.2	-3.9

Supplementary Figure 3 Identification of miRNAs in common between CREB shRNA and ADAR1 shRNA arrays. **(A)** Venn diagram showing the breakdown of the differentially regulated miRNAs between the two arrays analyzed. **(B)** Table of the 12 miRNAs identified to be in common between both the CREB shRNA and the ADAR1 shRNA array.



Supplementary Figure 4 miR-378-3p and miR-324-5p are edited by ADAR1 at one A-to-I editing site. **(A)** Mature miR-378 sequence highlighted in green. The arrow indicates the RNA editing site. **(B)** DNA sequencing data indicates a decrease in A-to-I editing in SB2 cells when ADAR1 is silenced. **(C)** An increase in RNA editing in C8161 cells is observed when ADAR1 is overexpressed. **(D)** A-to-I RNA editing is increased upon CREB silencing and is returned to NT levels upon rescue of CREB in C8161 cells. Editing sites

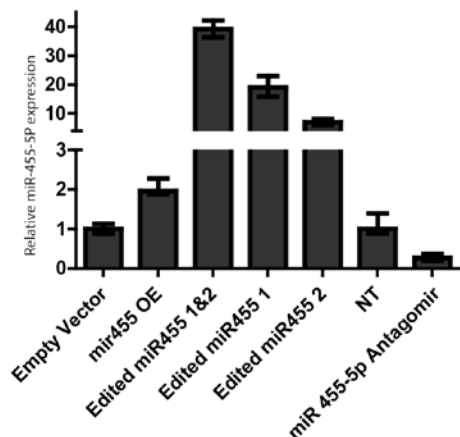
are indicated by a red arrow. **(E)** Mature miR-324 sequence is highlighted in green. The arrow indicates the RNA editing site. **(F)** DNA sequencing data indicates a decrease in A-to-I editing in SB2 cells when ADAR1 is silenced. **(G)** An increase in RNA editing is observed in C8161 cells when ADAR1 is overexpressed. **(H)** A-to-I RNA editing is increased upon CREB silencing and is returned to NT levels upon rescue of CREB in C8161 cells. Editing sites are indicated by a red arrow.



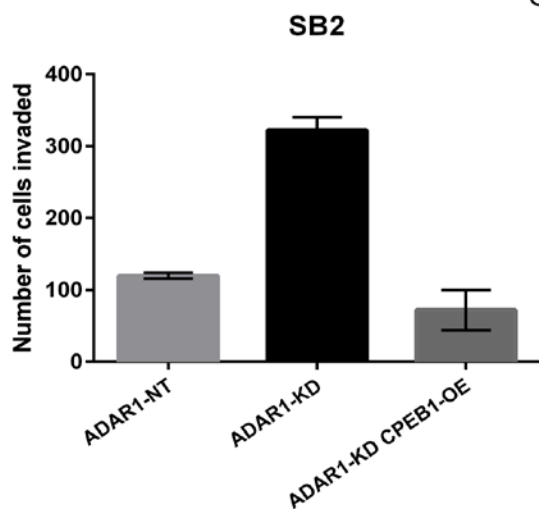
Supplementary Figure 5 Bound miR-455 to Drosha and Dicer correlates with ADAR1 expression. **(A)** Silencing ADAR1 in SB2 melanoma cells results in increased binding of mir-455 to Dicer, **(B)** Overexpressing ADAR1 in C8161 melanoma cells reduced the binding of mir-455 to Dicer. **(C)** Overexpression of ADAR1 in C8161 melanoma cells reduced

the amount of pri-miR-455 bound to Drosha. **(D)** Silencing ADAR1 in SB2 melanoma cells resulted with increased interaction between pri-miR-455 and Drosha (n=3 biologically independent samples; statistical significance by two-tailed Student t-test; error bars represent s.d., p<0.05).

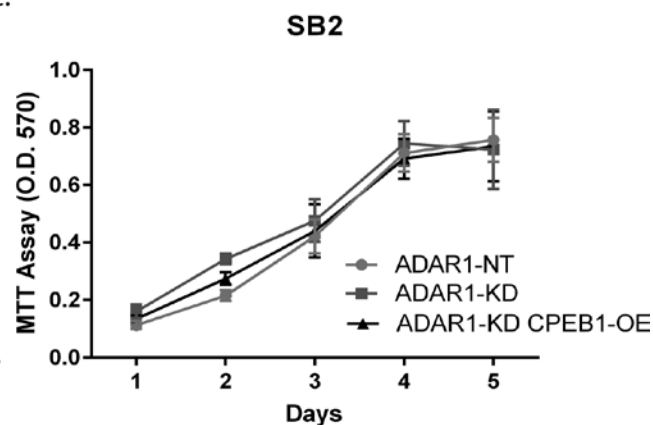
A.



B.



C.



Supplementary Figure 6 Confirmation of manipulation of miR-455-5p levels (A) rtPCR analysis of miR-455-5p levels show that wild-type miR-455-5p is overexpressed 2 fold, edited1 miR-455-5p is overexpressed ~20 fold, edited2 miR-455-5p is overexpressed ~9 fold and double edited miR-455-5p is overexpressed ~40 fold, as compared to empty vector control. The antagomir to miR-455-5p shows a downregulation of miR-455-5p by about 90% as compared to the NT control (n=3 biologically independent samples; statistical significance was determined by two-tailed Student t-test; error bars represent

s.d., $p < 0.05$). (B) Rescue of CPEB1 expression in SB2 ADAR1 KD cells inhibits their invasive potential in matrigel invasion assay, without affecting their proliferation rate (n=3 biologically independent samples; statistical significance was determined by Tukey's multiple comparison test; error bars represent s.d., $p < 0.05$). (C) No change was observed in proliferation rate between SB2 cells transfected with ADAR1-NT, ADAR1-KD, and ADAR1-KD CPEB1-OE (n=12 biologically independent samples per group. Statistical significance was determined by one-way ANOVA; error bars represent s.d., $p = 0.9610$). sa

ITGA2

5'-GCCAATTTATTATAGT**CACACA**-3' 3'UTR
 | | | | | | | |
 3'-GCTACGTCAGGTTT**CCGTGTGT**-5' EDITED miR455

5'-TTAATATT**CAATTTGCACACA**-3' 3'UTR
 | | | | | | | |
 3'-GCTACGTCAGGTTT**CCGTGTGT**-5' EDITED miR455

MDM4

5'-TTTTAATTCAGATAAA**CACACA**-3' 3'UTR
 | | | | | | | |
 3'-GCTACGTCAGGTTT**CCGTGTGT**-5' EDITED miR455

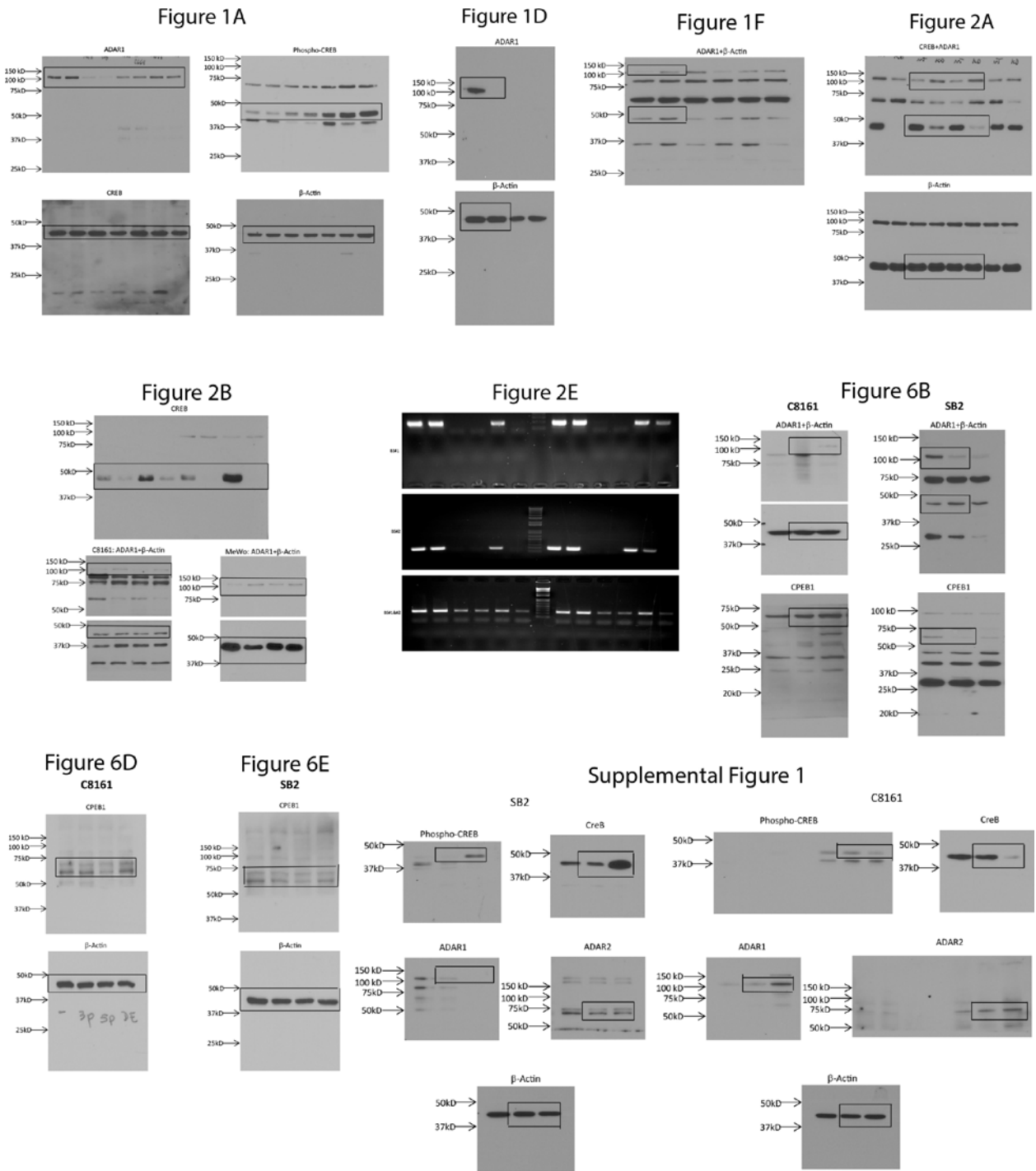
5'-AAGAATTGCTTGGACC**CACACA**-3' 3'UTR
 | | | | | | | |
 3'-GCTACGTCAGGTTT**CCGTGTGT**-5' EDITED miR455

5'-TCCTGACCTCATGAT**CACACA**-3' 3'UTR
 | | | | | | | |
 3'-GCTACGTCAGGTTT**CCGTGTGT**-5' EDITED miR455

RHOC

5'-TTCCC**CAAAGGATGGTCACACA**-3' 3'UTR
 | | | | | | | |
 3'-GCTACGTCAGGTTT**CCGTGTGT**-5' EDITED miR455

Supplementary Figure 7 Potential edited miR-455-5p binding sites on 3'UTR of ITG α 2, MDM4 and RhoC. miR-455-5p seed sequence is depicted in red and the edited sites are shown in green. 6-mer or 7-mer binding sites are highlighted in yellow.



Supplementary Figure 8 Uncropped Western blots and gel images.

Supplementary Table Legends

Supplementary Table 1 List of miRNAs differentially regulated after CREB silencing. miRNAs identified in both the CREB shRNA array and the ADAR1 shRNA array are highlighted in yellow.

Supplementary Table 2 List of genes identified from miR-455-5p microarray after ingenuity pathway analysis for cancer related genes. Genes highlighted in red are known oncogenes. Genes highlighted in green are known tumor suppressors.